Nontraumatic Intracranial Hemorrhage

Merve Gürsoy, Raffaella Basilico, and Cem Çalli

Contents

1 Nontraumatic Intracranial Hemorrhage

Nontraumatic intracranial hemorrhage (ICH) accounts for 10–15% of all strokes. Although the incidence of ischemic stroke is decreasing globally, the incidence of ICH is increased in older adults in association with the use of oral anticoagulants (Flaherty et al. 2007; Bejot et al. 2013). In addition, there has been significant improve-

ment in the management of and treatments for ischemic stroke, whereas the same is not applicable to ICH, which is still associated with high mortality and morbidity. ICH case fatality rate in the first month exceeds 50%, and only 20% of the survivors achieve full functional recovery within 6 months (van Asch et al. 2010).

Nontraumatic (spontaneous) ICH may be linked to many causes, and it is important to know the anatomic localization of the bleeding in order to reveal the underlying cause. The term ICH refers to bleeding into the brain parenchyma. However, bleeding may also extend to the subarachnoid space, subdural space, intraventricular space, or rarely to the epidural space. ICH can be classified as deep, lobar, and posterior fossa according to its localization. Deep ICH is the most common type, whereas posterior fossa is the rarest localization of ICH. Localization of the bleeding, patient's age, and clinical history (use

M. Gürsoy
Faculty of Medicine, Department of Radiology, Izmir Katip Celebi University, Izmir, Turkey

R. Basilico
Department of Neuroscience, Imaging and Clinical Sciencfves, Ss Annunziata Hospital "G. d'Annunzio" University, Chieti, Italy

C. Çalli (✉)
Department of Radiology, Ege University Medical School, Izmir, Turkey

of oral anticoagulants, hypertension, etc.) help narrow down the list of differential diagnoses that may be the cause of bleeding. The most common causes of nontraumatic ICH are hypertension and cerebral amyloid angiopathy (CAA) in older adults, and vascular anomaly and venous thrombosis in younger patients.

The first clinical manifestation of ICH is a sudden focal neurologic deficit which changes depending on the localization of the bleeding and frequently coexists with decreased level of consciousness, headache, and seizure. Hematomas expand in a few hours, and the clinical presentation progressively worsens in one-third of the patients with ICH (Delcourt et al. 2012). Therefore, prompt neuroimaging is critical. It was shown that the expansion of bleeding could be demonstrated better in patients who promptly undergo imaging (Fujii et al. 1998). Moreover, since the clinical findings of ischemic stroke and ICH are similar, neuroimaging is needed to distinguish between these 2 entities and to reveal the underlying cause.

2 Neuroimaging of ICH

Noncontrast computed tomography (CT), magnetic resonance imaging (MRI), and digital subtraction angiography (DSA) are frequently used to diagnose patients suspected of having ICH and to understand the cause of the condition.

2.1 Computed Tomography

Noncontrast CT is the primary imaging method of choice since it can be performed rapidly, showing bleeding with high sensitivity, and it is easily accessible in an emergency room setting. Noncontrast CT can both show the presence of bleeding and help evaluate the localization and size of the bleeding, presence of intraventricular hemorrhage as well as edema and mass effect that coexist with the hemorrhage. Blood may appear hyperdense on CT within a few minutes after extravasating from the vessel. Approximately after the third day, attenuation values of the clot

start to drop and it becomes isodense within a few weeks (Fig. 1). Therefore, while CT and MRI can show acute bleeding with similar sensitivity, MRI is superior to CT in showing chronic bleeding (Kidwell et al. 2004). In intraparenchymal hemorrhage, a hypodense area is observed around the hyperdense bleeding and it is caused by the serum from the retracted clot. The mentioned hypodensity reaches its maximum on day 5 with added vasogenic edema. Chronic hematomas appear as hypodense areas. Residual hypodensity, calcification, or slit-like lesions can be observed or there can be no signs on CT scans after the hemorrhage (Kreel et al. 1991).

CT angiography (CTA) is routinely performed at many centers along with CT in patients who are clinically suspected of having ICH or following the demonstration of hemorrhage with CT. CTA is especially recommended for young patients who have lobar hemorrhage without history of hypertension (Hemphill 3rd et al. 2015). In this patient group, CTA can help identify the cause of bleeding by showing vascular anomalies that frequently cause hemorrhage. Moreover, CTA may show the presence of "spot sign" on source images. Spot sign is defined as foci enhancement of 1–2 mm size in hematoma and implies active bleeding. Presence of a spot sign is an independent predictor of hematoma expansion and poor prognosis (Fig. 2) (Wada et al. 2007; Demchuk et al. 2012). Early hemostatic therapy (recombinant factor VIIa) was shown to potentially improve the prognosis of ICH by preventing the expansion of hematomas. However, the importance of spot sign in terms of showing which patients can benefit from hemostatic therapy and its exact role in treatment management remains to be demonstrated.

2.2 Magnetic Resonance Imaging

MRI is more sensitive than CT, especially for hemorrhages localized in the brain stem and posterior fossa as well as microbleeds associated with cerebral amyloid angiopathy (CAA) and hypertension. Appearance of blood on MRI is more complex than on CT scans, and the findings
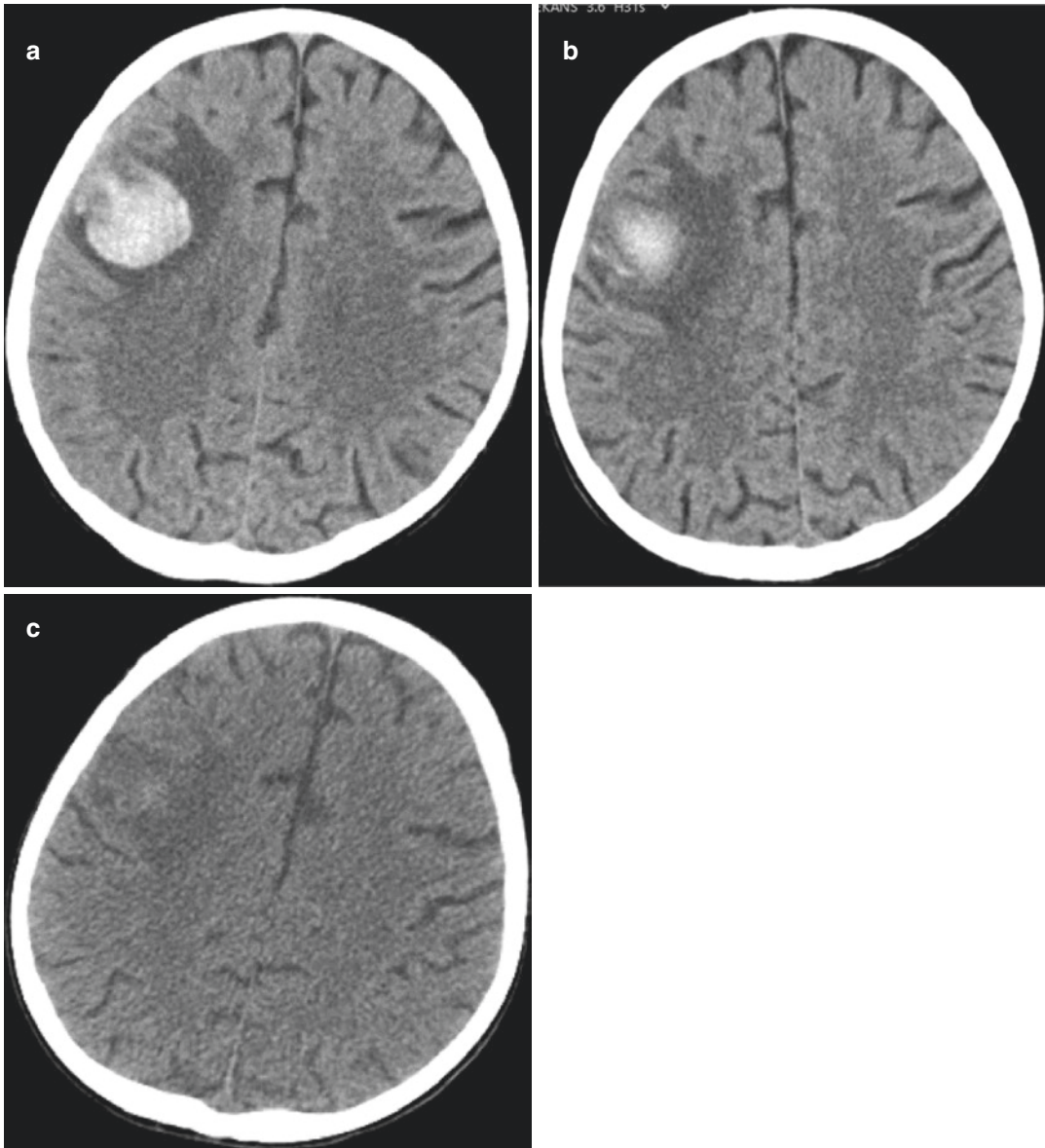
Fig. 1 Left frontal acute hematoma. (**a**) Hematoma appears hyperdense on first admission. (**b**) The density of hematoma decreases on day eighth with increasing diameter of peripheral edema. (**c**) On day 19th, the hematoma is almost isodense to cerebral parenchyma with continuation of peripheral edema

of imaging vary depending on the stage of bleeding and MRI sequence (Table 1). The variability of the findings depending on stage stem from the transformation of blood products from oxyhemoglobin to hemosiderin and ferritin.

Susceptibility-weighted imaging (SWI) is a modality that combines $T2^*$ imaging and phase information to detect products that change the intensity of the local magnetic field (Haacke et al. 2009). Blood products such as ferritin and hemosiderin have paramagnetic nature that changes the intensity of an external magnetic field and they appear as signal loss on SWI. SWI is significantly superior to the standard gradient recalled echo (GRE) sequence in detecting hemorrhage in the brain (Wycliffe et al. 2004).
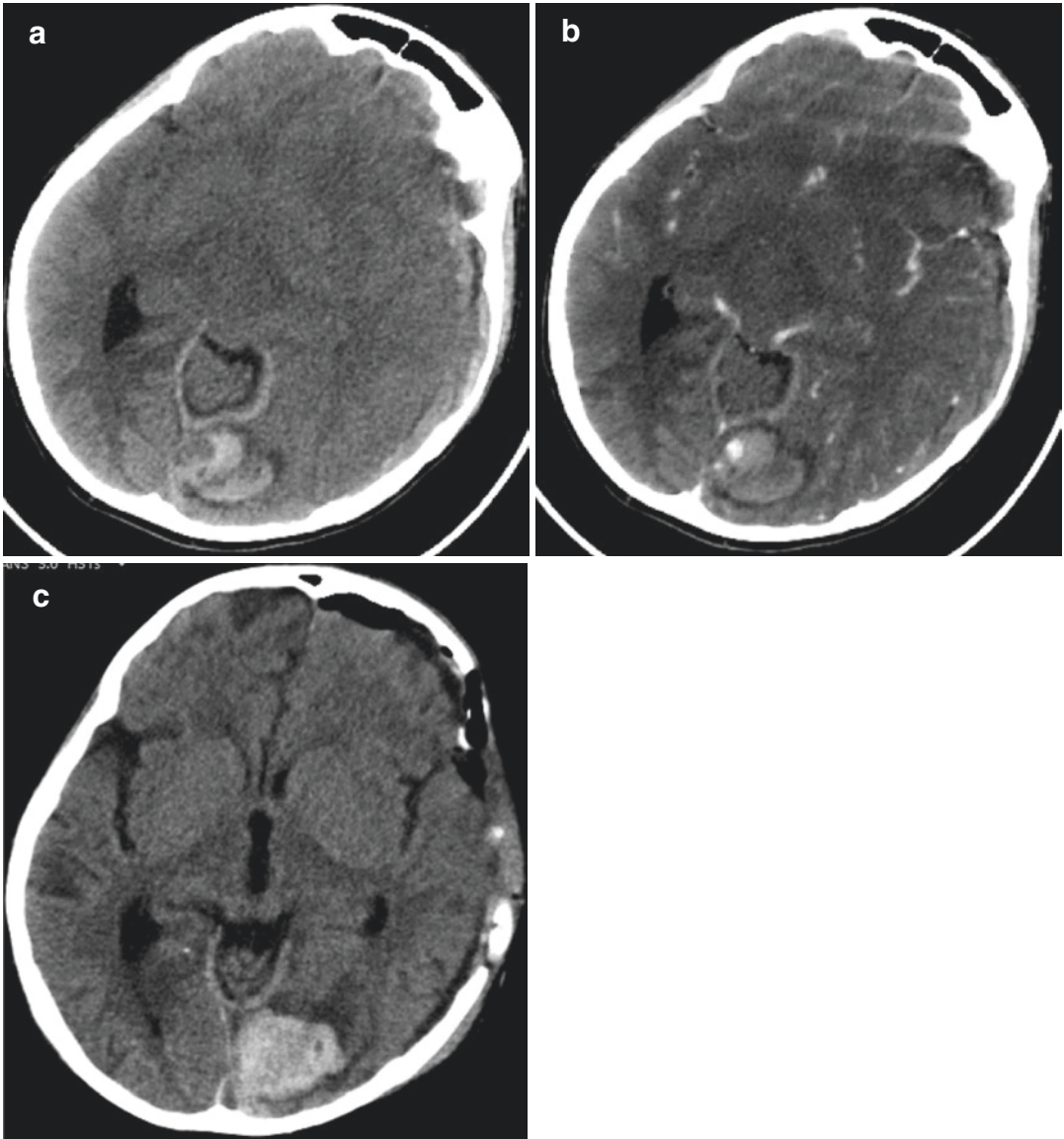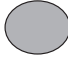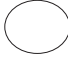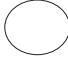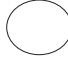
Fig. 2 Hematoma and the "Spot sign". (**a**) Left occipital hematoma is depicted on pre-contrast CT image. (**b**) CTA in the same session shows nodular focal enhancement inside the hematoma, so called "Spot sign" which predicts further hematoma growth. (**c**) CT examination after 2 days proves the increase in size of the hematoma

Another method that is used in neurovascular imaging and that employs a GRE sequence is time-of-flight MR angiography (TOF MRA). It utilizes flow-related enhancement. TOF MRA has high sensitivity for evaluating flow dynamics and detecting vascular lesions, and it does not require a contrast, which is the best advantage of this method.

MRI with diffusion-weighted imaging (DWI) is highly useful in detecting hemorrhagic transformation of ischemic stroke. The location and size of the infarct underlying the bleeding which can be overlooked in noncontrast CT can be clearly determined with DWI. However, emergency MRI cannot be performed in many cases due to limited time, costs, and patients who cannot tolerate the test.

Table 1 MRI Signal Characteristics and CT appearance of Different Stages of Intracranial Hemorrhage (Figs. 3, 4, 5, and 6)

Stage	Phase of hemoglobin	CT	T1WI	T2WI
Hyperacute (<12 h)	Oxyhemoglobin	High density (high protein)	Isointense to hypointense	Hyperintense with hypointense rim
Acute (12 h to 3 days)	Deoxyhemoglobin	High density (high protein)	Isointense	Hypointense
Early subacute (3–7 days)	Intracellular methemoglobin	High density (high protein)	Hyperintense	Hypointense
Late subacute (7–14 days)	Extracellular methemoglobin	Isodense (absorption of high protein)	Hyperintense	Hyperintense
Chronic (>2 weeks)	Hemosiderin and ferritin	Low density (atrophy)	Hypointense	Hypointense

MRI magnetic resonance imaging, *CT* computed tomography, *T1WI* T1-weighted image, *T2WI* T2-weighted image

Hypointense ⬤ Isointense 🔘 Hyperintense ◯
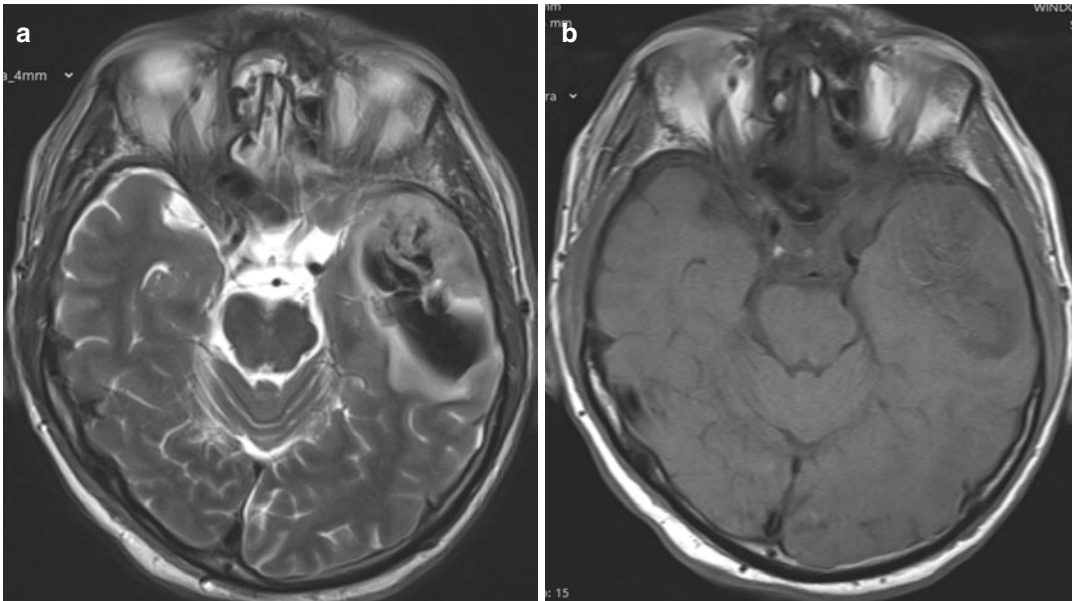
Fig. 3 Acute hematoma. (**a**) T2W image depicts hypointensity and (**b**) T1W image shows iso-hypointensity in left temporal acute stage hematoma
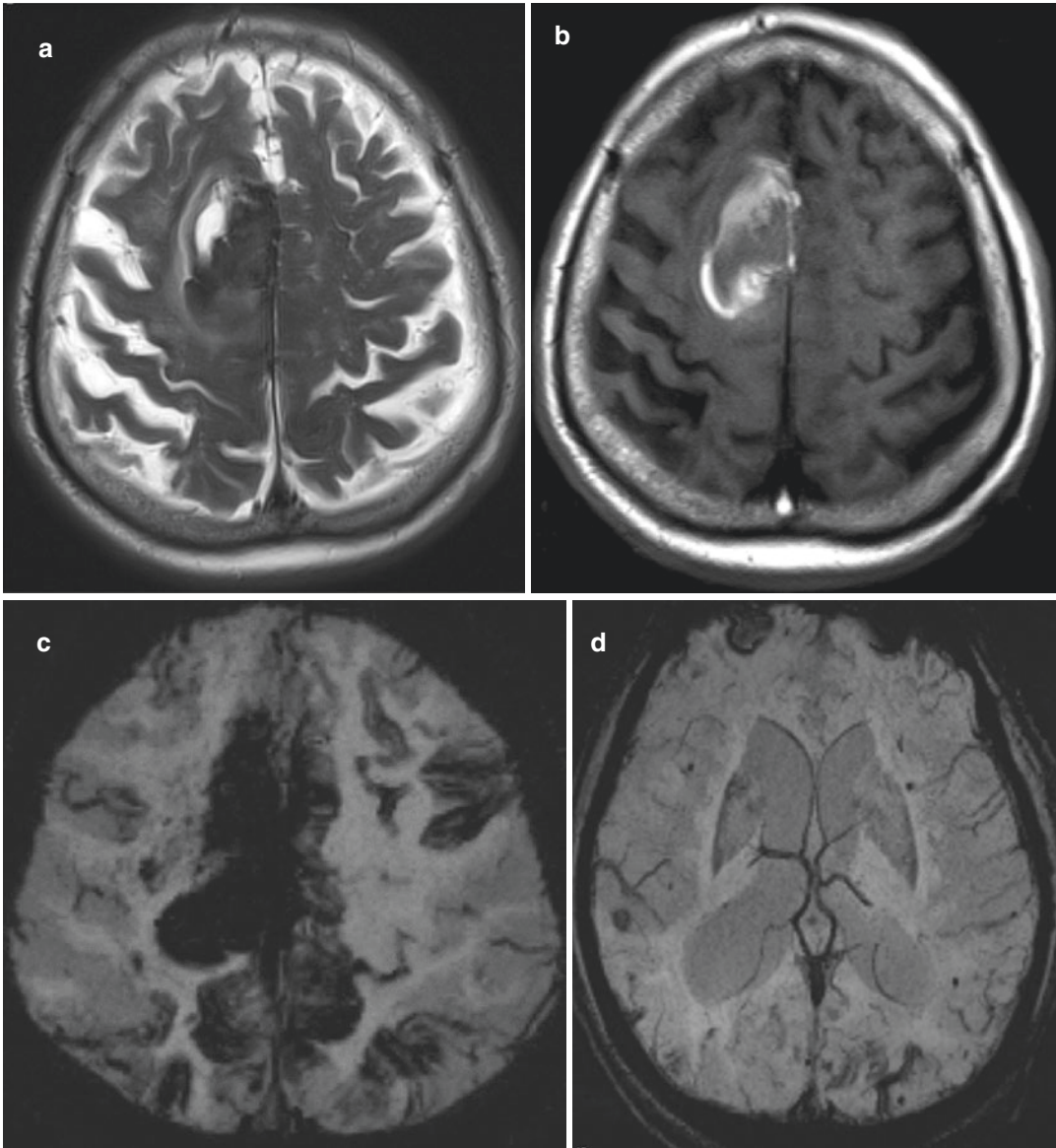
Fig. 4 Early subacute hematoma. The right frontal lobar hematoma reveals hypointensity on T2W image (**a**) and peripheral hyperintensity on T1W image (**b**). (**c**) SWI image shows marked hypointensity in the lesion as well as multiple subcortical nodular and sulcal hypointensities consistent with CAA. (**d**) SWI image at more caudal level does not reveal microbleeds in basal ganglia

2.3 Digital Subtraction Angiography

Despite the advanced examination methods and developments in neuroimaging, digital subtraction angiography (DSA) is still used in certain patients to identify the cause of ICH. It was shown that the localization of bleeding, patient's age, and history of hypertension were important factors that had an impact on the possibility of detecting vascular anomalies with cerebral angiography in nontraumatic (spontaneous) ICH (Xhu et al. 1997). DSA is recommended for patients under 45 who do not have history of
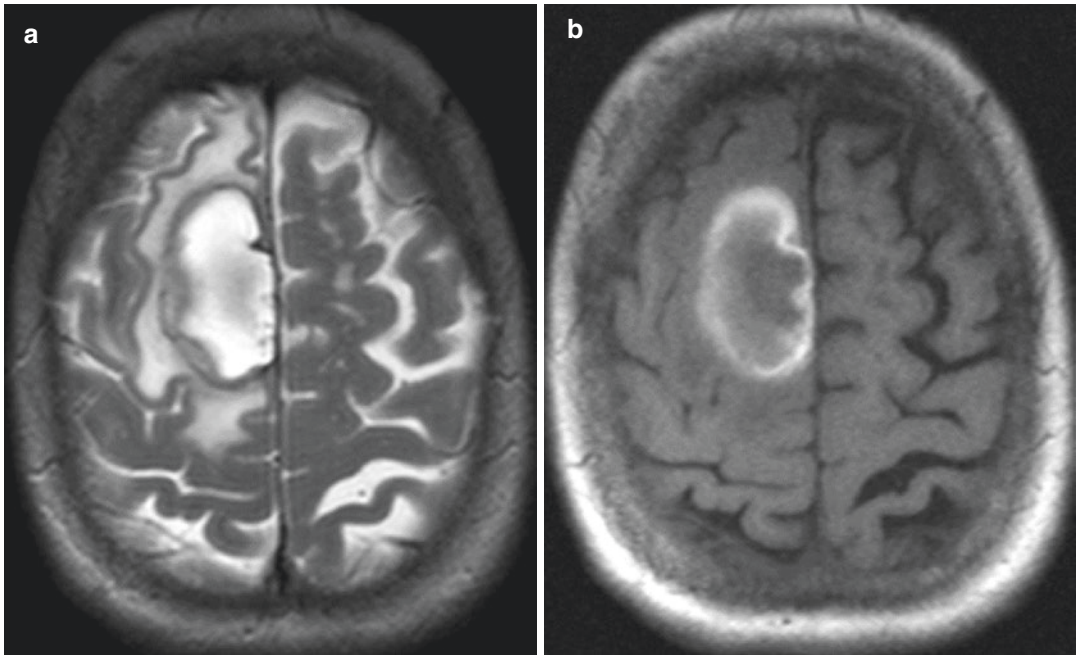
Fig. 5 Late subacute hematoma. Right frontal lobar hematoma shows hyperintensity on both T2W (**a**) and T1W images (**b**)
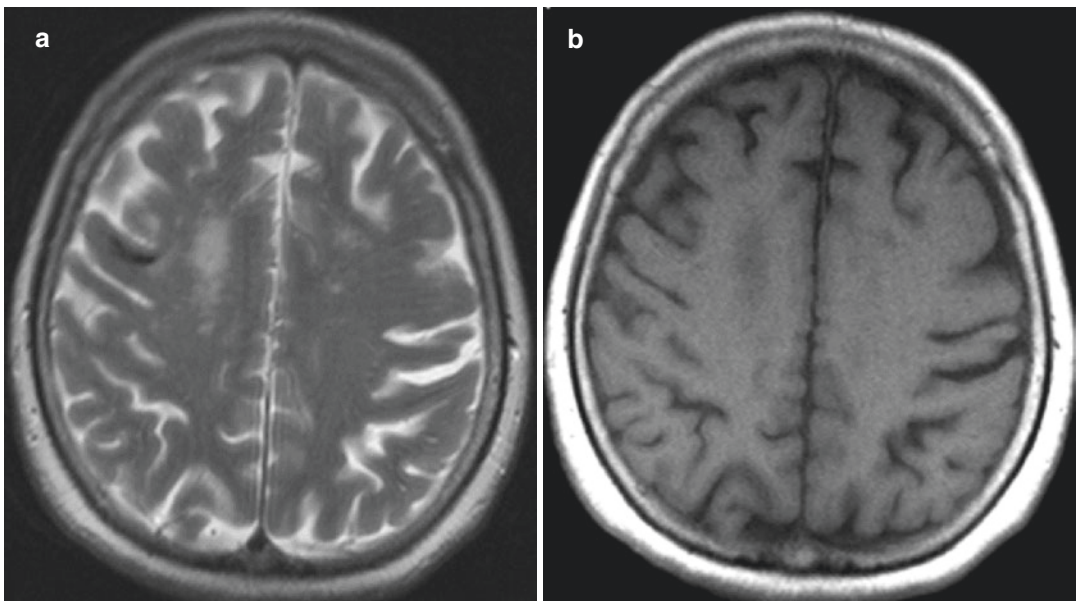
Fig. 6 Chronic hematoma. There is a linear hypointensity at right frontal subcortical white matter on T2W image (**a**), which is also hypointense on T1W image (**b**)

hypertension and have lobar hemorrhage if the cause of bleeding cannot be identified with non-invasive methods or for patients above 45 if the cause of bleeding cannot be identified with SWI and contrast MRI.

3 Causes of Nontraumatic Intracerebral Hemorrhage

ICH is traditionally classified as traumatic and nontraumatic (spontaneous), wherein nontraumatic ICH is classified as primary and secondary depending on the cause of hemorrhage. The term primary ICH is used for CAA and hypertension that involve cerebral small vessels and primary ICHs constitute the majority of nontraumatic ICHs (78–88%) (Foulkes et al. 1988). In addition, secondary ICH encompasses hemorrhages with an apparent underlying cause such as coagulopathy, vascular lesion, tumor, or venous sinus thrombosis (Table 2). Therefore, knowing the localization of hemorrhage (lobar, deep, posterior fossa), clinical history (hypertension, use of oral anticoagulants), and patient's age is essential to narrow down this considerably long list of differential diagnoses.

Table 2 Classification of nontraumatic intracranial hemorrhage according to causes

Causes	Characteristics
Primary	
Hypertension	Most common reason, deep location, clinical history of hypertension
Amyloid angiopathy	Lobar, cortical-subcortical location, older patients, high recurrence
Secondary	
Vascular malformations • Cavernous angioma. • Arteriovenous malformation.	Young adults, need for imaging studies such as CTA/MRA and DSA
Venous thrombosis	Noncompliance with arterial distribution, bleeding near the dural venous sinus or deep cerebral vein, empty delta sign.
Nontraumatic subarachnoid hemorrhage	Ruptured aneurysm, the most severe headache in patient's life, sulcal hyperintensity on FLAIR is sensitive but not specific.
Coagulopathy • Use of anticoagulants. • Congenital (antithrombin III, protein C, protein S, von Willebrand, factor VII, IX, VII deficiency). • Acquired (thrombocytopenia, DIC, uremia, MM, leukemia).	Most commonly associated with use of anticoagulants. The clinical history is important to prevent continued bleeding.
Neoplasm • Primary (grade III, IV astrocytoma). • Metastasis.	Mostly malign, contrast-enhanced MRI is useful for diagnosis. Recurrence of hemorrhage is common.
Hemorrhagic transformation of ischemic stroke	DWI is useful in demonstrating the ischemia underlying bleeding.
Vasculitis/vasculopathy	Serological examination of CSF or brain biopsy is required for certain diagnosis.
Infection	Other signs of infection (fever, elevated ESR, and CRP), hemorrhage due to vasculitis, coagulopathy, septic embolism, or microbial aneurysm.
Alcohol and drugs • Cocaine. • Amphetamine.	Due to acute (drugs) or chronic (alcohol) elevation of hypertension. Concomitant pathologies (aneurysm, AVM) may be present in drug-associated ICH.

MRI magnetic resonance imaging, *DSA* digital subtraction angiography, *DWI* diffusion-weighted imaging, *DIC* disseminated intravascular coagulopathy, *MM* multiple myeloma, *CSF* cerebrospinal fluid, *ESR* erythrocyte sedimentation rate, *CRP* C-reactive protein, *ICH* intracranial hemorrhage

3.1 Primary Nontraumatic Intracranial Hemorrhage

3.1.1 Hypertension

Chronic hypertension is the leading cause of primary ICH. Long-term hypertension causes reactive hyperplasia in the deep-penetrating arterioles that originate from the anterior, middle, or posterior cerebral arteries and basilar artery in the brain. This leads to lipohyalinosis and fibrinoid necrosis on arteriole walls. As a result of these degenerative changes, compliance decreases, and the arteriole becomes prone to rupture. It was previously thought that hemorrhages due to hypertension originated from microscopic aneurysms that are called Charcot-Bouchard aneurysms. However, it was then understood that such hemorrhages were extravascular clots that stemmed from endothelial damage or subadventitial hemorrhages (Fisher 1971).

Hypertensive ICH is typically observed in the putamen and internal capsule (60–65%), thalamus (15–25%), and pons (5–10%) (Osborn 1994). Localization of hemorrhage reflects the watershed areas of the affected deep perforating arteries. Lobar location is rarer and accounts for 10% of the cases. It is thought that lobar hemorrhage can stem from CAA which can be observed with hypertension especially in older patients (Pantoni 2010). Neuroimaging shows other signs of hypertension in the brain in addition to hemorrhage due to hypertension (Fig. 7). Although small arterioles are generally beyond the resolution of MRI, their complex effects on the brain can still be visualized. The key MRI findings associated with small vessel disease consist of cerebral microbleeds and leukoaraiosis (white matter changes). Cerebral microbleeds appear as small, homogenous, and round- or oval-shaped hypointense foci on images obtained by T2*-weighted GRE and SWI. Leukoaraiosis appears
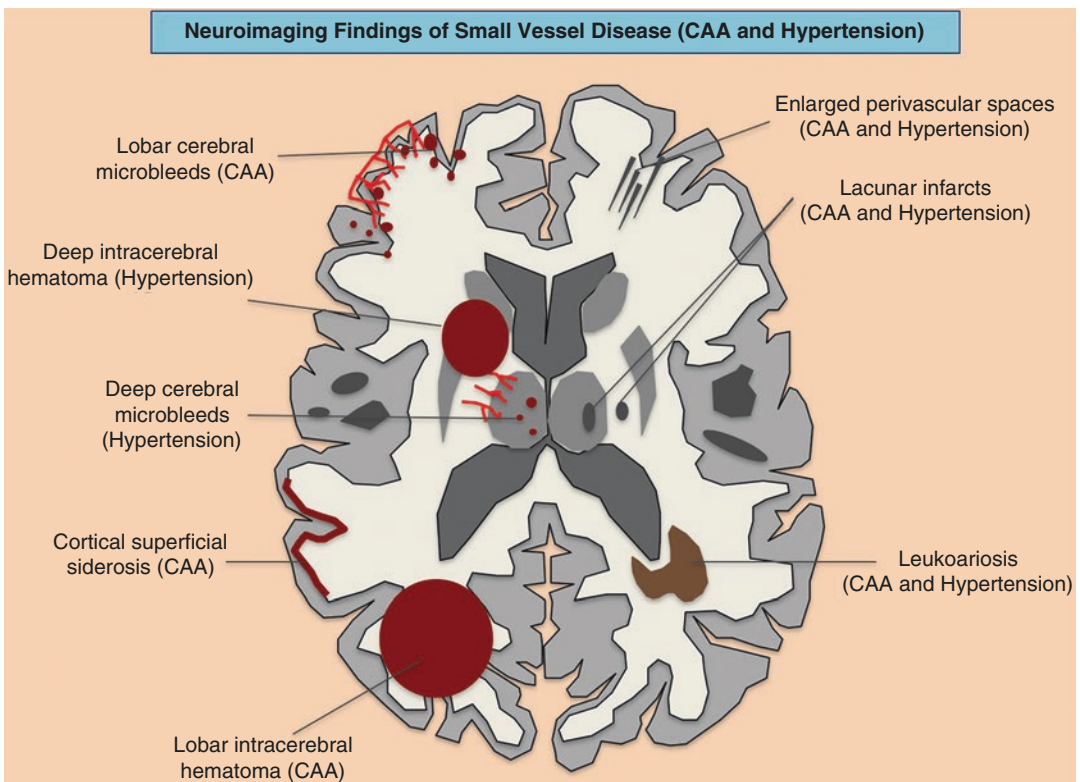
Fig. 7 Schematic drawing shows neuroimaging findings of small vessel disease. *CAA*: cerebral amyloid angiopathy
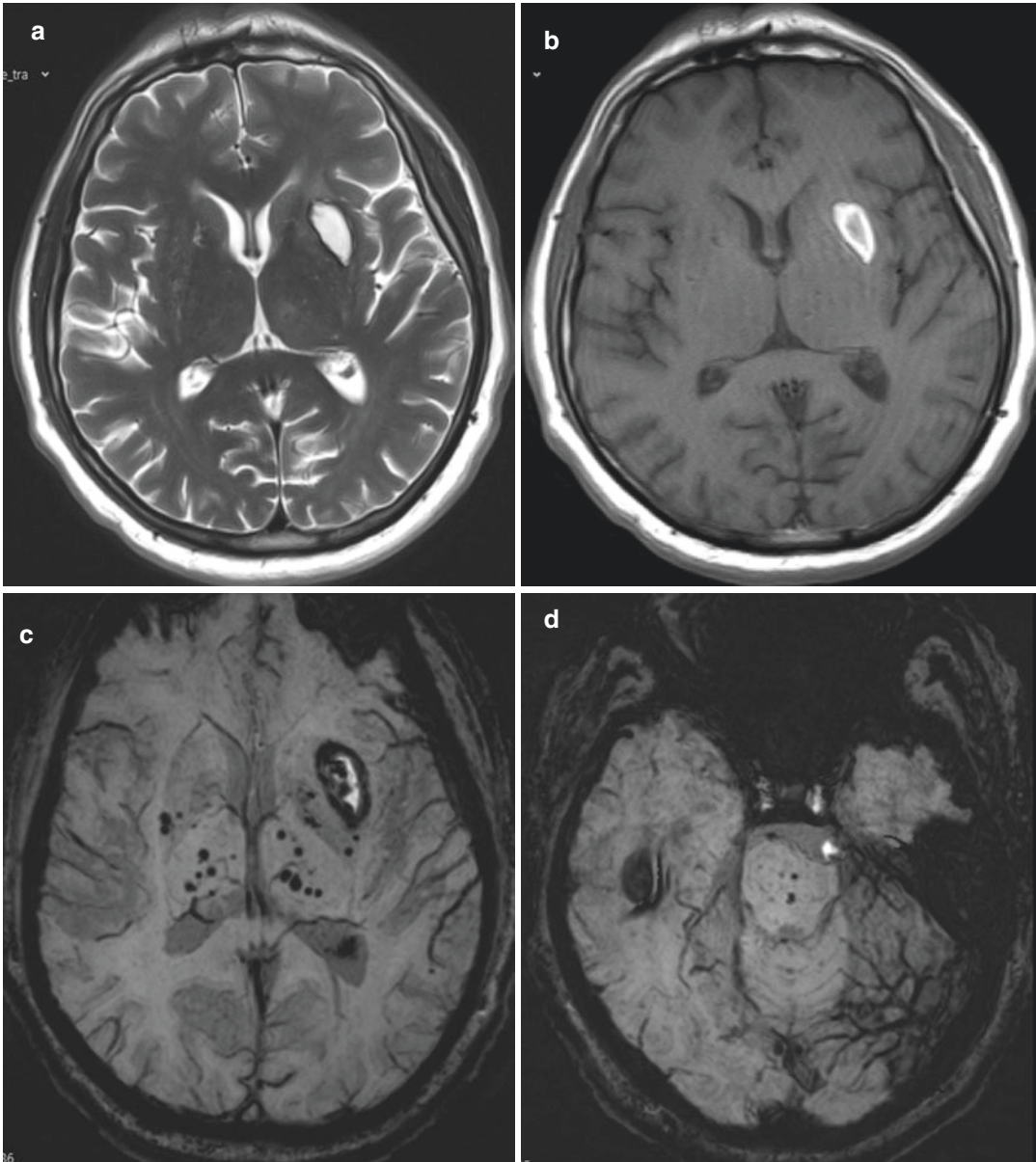
Fig. 8 Hypertensive hematoma. There is left putaminal late subacute focal hematoma which is hyperintense both on T2W (**a**) and on T1W (**b**) images. (**c**, **d**) SWI images depict multiple microbleeds in basal ganglia and thalami as well as in the brainstem consistent with chronic hypertensive encephalopathy

as confluent hyperintense areas on images obtained with T2WI and FLAIR. Localization of leukoaraiosis is not a useful marker to determine the underlying cause of small vessel disease (Smith et al. 2010). However, localization of cerebral microbleeds is useful in determining the underlying cause of hemorrhage. Hypertension should be considered as the underlying cause of hematoma in patients above 45, when there are microvascular white matter changes on T2W1 and FLAIR as well as deep microbleeds at locations of basal ganglia and brainstem (Fig. 8). In addition, lobar microbleeds are strongly associated with CAA. Another neuroimaging finding in

small vessel disease is lacunar infarcts. While lacunar infarcts associated with hypertension are localized in deep gray matter like in microbleeds, lacunar infarcts linked to CAA are localized in centrum semiovale and lobar regions.

More than one in three intraparenchymal hematomas expand within 24–36 h. It was shown that the possibility of hematoma expansion was higher in those who underwent the first CT sooner, used oral anticoagulants, and had larger hematomas (Brott et al. 1997). Therefore, it should be kept in mind that the mass effect, which is lower initially, will also increase with expanding hematoma and increasing edema.

3.1.2 Cerebral Amyloid Angiopathy

CAA is a small vessel disease in which progressive β-amyloid protein build-up is observed on the walls of superficial small and mid-sized vessels in the leptomeninges and cerebral cortex. The affected vessels exhibit wall thickening, microaneurysms, and fibrinoid degeneration. The vessels become prone to rupture and luminal occlusion can also be observed in vessels. ICH develops when the vessel ruptures, whereas ischemia and leukoencephalopathy develop when there is occlusion.

The prevalence of CAA increases with age (particularly >60 years), but most of these patients are asymptomatic. Autopsy studies have shown that more than 70% of the asymptomatic population older than 90 had CAA (Tanskanen et al. 2012).

The definitive diagnosis of CAA is made by histopathological examination of the tissue. However, neuroimaging is critical, since such histopathological examination is not possible most of the time. Therefore, Boston criteria that include imaging findings were described in order to standardize the diagnosis of CAA (Table 3) (Knudsen et al. 2001). While CAA can be asymptomatic with cerebral microbleeds and white matter changes, it can also lead to symptomatic ICH. Cerebral microbleeds associated with CAA typically have cortical and subcortical localization unlike the deep localization in hypertension.

Table 3 Boston criteria for the diagnosis of CAA in patients with intracranial hemorrhage

Category	Description
Definite CAA	Postmortem examination • Lobar, cortical, or corticosubcortical hemorrhage. • Severe CAA. • Absence of another cause.
Probable CAA with supporting pathology	Clinical data and pathologic tissue • Lobar, cortical, or corticosubcortical hemorrhage. • Some amyloid deposition in specimen. • Absence of another cause.
Probable CAA	Clinical data and MRI • Multiple lobar, cortical, or corticosubcortical hemorrhages. • Age >55 years. • Absence of another cause.
Possible CAA	Clinical data and MRI • Single lobar, cortical, or corticosubcortical hemorrhage. • Age >55 years. • Absence of another cause.

CAA cerebral amyloid angiopathy, *MRI* magnetic resonance imaging

In general, there are multiple hemorrhages that tend to recur. CAA should be considered in patients older than 55 who have microbleeds localized in the cortical and corticomedullary junction without history of hypertension. CAA-related ICH accounts for 5–20% of all nontraumatic ICHs (Maia et al. 2007). Symptomatic parenchymal hemorrhage most frequently occurs in the frontal and parietal lobes, cortex, and subcortical regions and extends to the subarachnoid and rarely to the subdural space. Hemorrhage can also be observed in the cerebellum, although rare. Symptomatic hemorrhages are larger than microbleeds (>5 mm). Another rare sign associated with CAA is cortical superficial siderosis. It is a progressive disease caused by chronic recurrent subarachnoid hemorrhage and is characterized by the deposition of hemosiderin on pial surfaces of the central nervous system (CNS). The imaging shows hypointensity, especially marked in SWI, covering the surface of the brain (Fig. 4).

It was shown that hypertension, higher number of cerebral microbleeds, and anticoagulant use increased the risk of hemorrhage in CAA (Rosand et al. 2000; Greenberg et al. 2004). Therefore, the risks and benefits should be assessed, and the treatment should be personalized in patients who need to use anticoagulants for some other reason.

3.2 Secondary Nontraumatic Intracranial Hemorrhage

3.2.1 Vascular Malformations

Vascular malformations represent a large group of pathologies including arteriovenous malformation (AVM), cavernous malformation (CM), dural arteriovenous fistulas (dAVFs), developmental venous anomaly (DVA), and capillary telangiectasia. DVA and capillary telangiectasia are common, but they frequently do not cause hemorrhage, whereas AVM and CM have a higher potential to cause hemorrhage. In addition, dAVF rarely causes bleeding.

Vascular malformation is the most common cause of nontraumatic ICH in young adults (Shahi and Warlow 2001). CTA can detect the underlying vascular malformation with 90% accuracy, after the presence of ICH has been demonstrated using CT (Romero et al. 2009; Yeung et al. 2009). The abnormal vessels can be directly visualized, similar to MRA. DSA is generally used to identify and treat small lesions that are not visible on CT and MRI.

AVM: AVM stems from abnormal connections between the arteries and veins. AVM consists of one or more feeding arteries, a bundle of blood vessels where the arterial blood is shunted called the nidus and enlarged draining veins. There may be an aneurysm in the feeding arteries and nidus. The feeding artery originates from the internal carotid artery or vertebrobasilar system. One in three ICHs occur due to AVM in young adults. AVMs that have not ruptured have 2–4% risk of hemorrhage per year, and this risk increases in recurrent hemorrhages (Al-Shahi and Warlow 2001). There are many morphological factors that are associated with hemorrhage in AVMs. It was shown that increasing age, deep brain localization, and exclusive deep venous drainage were independent predictors of hemorrhage in AVM (Stapf et al. 2006).

AVMs are generally asymptomatic, and they are detected incidentally on CT and MRI scans performed for other reasons. Noncontrast CT and MRI can generally detect an unruptured AVM. Enlarged draining veins can appear as slightly hyperdense areas in serpentine configuration on a noncontrast CT scan. This is generally accompanied by calcification and encephalomalacia surrounding the AVM. Contrast-enhanced CT may show curvilinear vascular structures with marked contrast uptake. MRI typically shows curvilinear flow voids in feeding arteries and draining veins. The nidus and enlarged vascular structures can be clearly visualized using CTA and MRA (particularly time-resolved enhanced MRA and CTA). When hemorrhage occurs in AVM, the bleeding may hinder the visualization of the AVM (Fig. 9). Calcification and enlarged vessels in the vicinity of the bleed may assist the diagnosis. In addition, small AVMs, especially when they are localized near the dural venous sinus, may not be visible on CT and MRI scans (since draining veins will travel a shorter path). Therefore, the definitive diagnosis of AVMs is made using DSA. However, a negative result from the first angiogram should not rule out an AVM, since the mass effect from the hematoma may prevent the visualization of small AVMs. Therefore, a second evaluation should be considered after the mass effect is removed, if there is clinical suspicion.

Transcatheter embolization, surgery, and stereotactic radiosurgery are used in the treatment of AVMs. A grading system has been described by Spetzler and Martin in order to predict the surgical outcome in AVMs. With this grading system, AVMs were classified and graded according to size, localization, and pattern of venous drainage (Table 4). A higher score means that the estimated surgical outcome is worse (Spetzler and Martin 1986).

CM: CMs are lesions that consist of thin-walled dilated venous channels lined by a single layer of endothelial cells. These vascular lesions
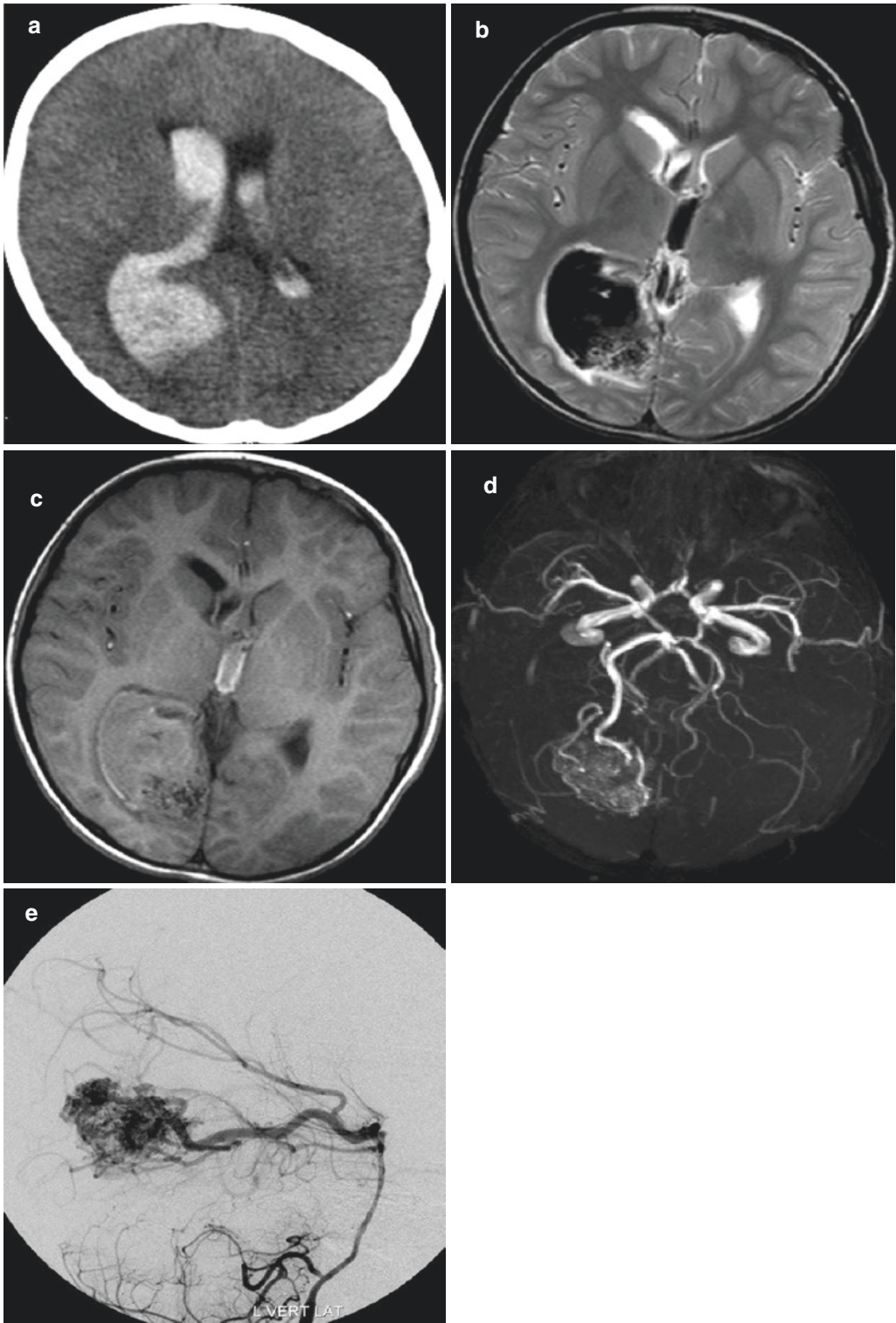
Fig. 9 AVM hemorrhage. (**a**) Noncontrast CT shows right occipital acute hematoma with extension to the ventricles. Hematoma is hypointense on T2W (**b**) and isointense on T1W (**c**) images. Note that subtle signal voids at the posterior aspect of the hematoma are seen. (**d**) 3D TOF MRA reveals abnormal arterial structures inside the hematoma consistent with AVM. Right posterior cerebral artery is dilated as the major feeding artery. (**e**) DSA proves the presence of an AVM

Table 4 Spetzler-Martin grading scale for arteriovenous malformations[a]

Graded Feature	Points Assigned
Size of AVM	
Small (<3 cm)	1
Medium (3 to 6 cm)	2
Large (>6 cm)	3
Eloquence of adjacent brain	
No	0
Yes	1
Venous drainage	
Superficial only	0
Deep	1

[a]Grade = size + eloquence + venous drainage
Data from Spetzler RF, Martin NA. A proposed grading system for arteriovenous malformation. J Neurosurg 1986;65:476e83

do not contain glial or neural tissue. CMs can be sporadic or familial. While there is a single lesion in the sporadic type, the familial type has multiple lesions. CMs can be associated with DVA or occur independently. Although CMs can be present at any region in the brain, they are generally located in the supratentorial region. CMs are generally asymptomatic and they are detected by chance on imaging tests performed for another indication, or patients present with an acute focal neurologic deficit or seizure due to hemorrhage. The annual hemorrhage rate of CMs is 2.5% per patient-year. Several risk factors (younger age, female sex, deep location, size, multiplicity, associated DVA, etc.) were defined for hemorrhage in CM in various studies. However, the results are controversial. The most well-known risk factor, among others, is history of CM hemorrhage (Gross and Du 2017). Hemorrhage rates for unruptured CMs are ranging from 0.4% to 0.6% per patient-year in the literature. Those for ruptured CM vary from 4.5% to 22.9% per patient-year (Gross and Du 2017).

CMs generally appear on CT scans as small, round-, or oval-shaped isodense lesions containing high-density areas. Edema and mass effect are not usually observed in the absence of hemorrhage. MRI should be the imaging method of choice in the diagnosis of CM. CMs are typically surrounded by a hypointense rim due to hemosiderin on T1WI and T2WI. The hypointense rim is more marked on SWI. In addition, sometimes, small CMs can only be visualized using the SWI sequence (Fig. 10). The signal at the center of the lesion varies depending on the stage of hemorrhage but it is generally a heterogenous signal (popcorn pattern) with hyperintense areas on T1WI and T2WI. There is usually a slight contrast uptake on postcontrast series. However, a contrast agent is mainly administered to detect a coexisting DVA. 8–33% of CM cases also have DVA (Rammos et al. 2009). Detection of a DVA is particularly useful for diagnosing CM, which is difficult to visualize in the presence of a hematoma. CMs are not visible on catheter angiography, which is not used for the diagnosis. Asymptomatic CMs are generally followed up in a conservative fashion. Surgical excision of the lesion or stereotactic radiosurgery is recommended for symptomatic cases due to the fact that recurrent hemorrhages may lead to permanent neurologic deficits. For patients who are planned to undergo surgery, a contrast-enhanced MRI should be performed before the treatment in order to detect an accompanying DVA and due to the risk of postoperative venous infarction.

dAVF: dAVF refers to an abnormal connection between the meningeal artery and meningeal vein or lumen of the dural venous sinus. It frequently occurs secondary to dural sinus thrombosis. On the other hand, dAVF may also be idiopathic, posttraumatic, secondary to craniotomy, or due to hormonal changes (pregnancy, use of oral contraceptives). It constitutes 10–15% of all intracranial vascular malformations (Newton and Cronqvist 1969). dAVF is most frequently observed at the cavernous sinus level or the cribriform plate or sigmoid sinus (Zipfel et al. 2009).

Clinical signs of dAVF depend on the localization of the lesion and the pattern of venous drainage (Tsai et al. 2004; Lucas Cde et al. 2006). The most distinct clinical presentation is observed in dAVFs that drain into the cavernous sinus. Proptosis, chemosis, ophthalmoplegia, and loss
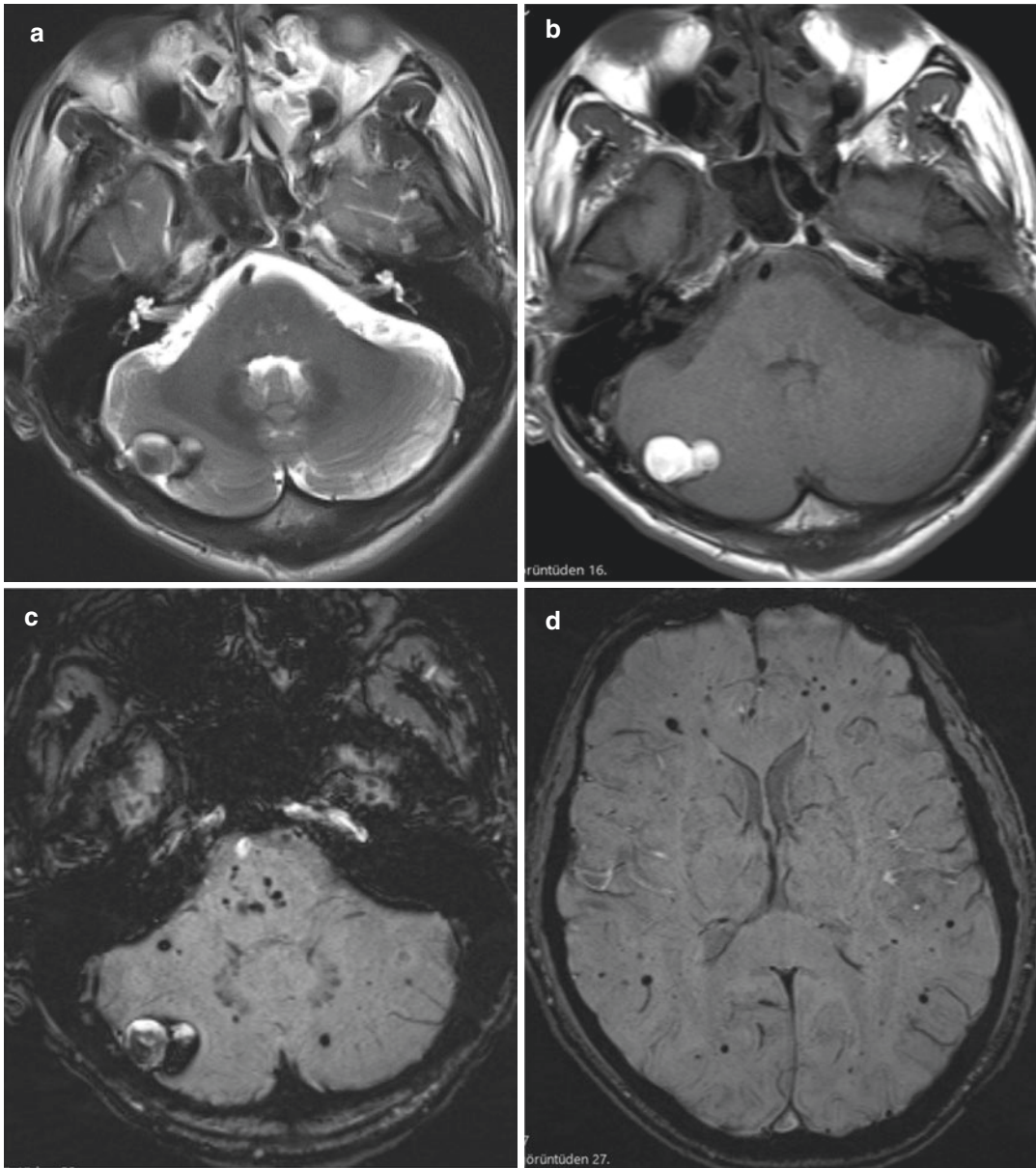
Fig. 10 Cavernoma. There is right cerebellar early subacute hematoma which is hypointense on T2W image (**a**) and also hyperintense on T1W image (**b**). (**c**, **d**) SWI images depict multiple tiny hypointense lesions representing multiple cavernomas, which cannot be detected on conventional images

of vision are typically observed. In addition, dAVFs in the transverse sigmoid junction typically exhibit pulsatile tinnitus. Headache secondary to venous hypertension and dementia as a result of cerebral hypoxia can also be observed. dAVF rarely causes bleeding. Hemorrhage stems from the increased pressure due to retrograde venous flow causing the rupture of parenchymal veins. Petrosal or straight sinus location, leptomeningeal venous drainage, and presence of varix in the draining vein increase the risk of hemorrhage.

dAVFs may appear completely normal on CT and MRI in the absence of dural venous sinus thrombosis, dilated cortical veins, hydrocephaly, or ICH. Tortuous feeding arteries, venous sinus occlusion, enlarged cortical veins can be clearly visualized on CTA and MRA/MR venography (MRV). DSA is the gold standard in diagnosis. A selective angiogram encompassing the bilateral internal carotid arteries, external carotid, and vertebral artery should be obtained. DSA can provide the diagnosis of the lesion in addition to the characterization of the arterial feeding vessels and pattern of venous drainage as well as enabling endovascular treatment of many lesions. Various grading systems were proposed for the grading of dAVFs. The Cognard and Borden classifications, based on the pattern of venous drainage, are the most commonly used systems (Cognard et al. 1995; Borden et al. 1995). A higher grade means more aggressive presentation and higher risk of hemorrhage (Table 5).

3.2.2 Venous Thrombosis

Venous thrombosis accounts for 0.5–1% of all strokes in the adult population (Saposnik et al. 2011). The incidence thereof is higher in the pediatric population and females (Coutinho et al.

2012). There are many risk factors that play a role in the etiology of venous thrombosis including thrombophilia (genetic or acquired), oral contraceptive use, pregnancy, dehydration (diarrhea in children), head trauma, malignancy, and infections. Clinical signs are not specific to venous thrombosis. The diagnosis may be delayed since symptoms such as headaches, seizures, papilledema, and focal neurologic deficits can be present in various pathologies. Headaches and papilledema, which can be observed in 40% of the patients, are associated with increased intracranial pressure.

39% of all venous thrombosis events are associated with hemorrhage (Ferro et al. 2004). It was shown that some factors such as pregnancy, thrombosis of a large sinus, and hypertension at admission were associated with intracerebral hemorrhage and poor prognosis (Kumral et al. 2012). Venous thrombosis should be considered as the underlying cause, especially when ICH is localized in certain regions such as the temporal lobe, parasagittal frontal or parietal lobe, bilateral thalami, and internal capsule. Noncontrast CT is the first diagnostic procedure as in all patients who present with nonspecific neurological symptoms. However, CTV or MRI/MRV should be

Table 5 Classification systems for cerebral dAVFs

| Cognard classification		Borden classification	
Type	Description	Type	Description
Type I	Anterograde drainage into venous sinus	Type I	Anterograde drainage into the dural sinus/ meningeal vein
Type II	Drainage into a sinus but with insufficient antegrade venous drainage and reflux.	Type II	Anterograde drainage into dural sinus and retrograde drainage into cortical veins
• Type IIa	Retrograde venous drainage into sinüs	Type III	Isolated retrograde drainage into cortical veins
• Type IIb	Retrograde venous drainage into cortical veins		
• Type IIa + IIb	Retrograde venous drainage into sinus and cortical veins		
Type III	Direct cortical venous drainage without ectasia		
Type IV	Direct cortical venous Drainage with venous Ectasia >5 mm and 3 times larger than the diameter of the draining vein		
Type V	Drainage into the spinal perimedullary veins		

performed promptly in the presence of findings that are suggestive of venous thrombosis on non-contrast CT scans. Indirect signs of venous thrombosis such as hemorrhage, if present, and brain edema can be observed on noncontrast CT images. Thrombosed dural venous sinus or cortical vein (cord sign) can appear hyperdense. However, this classical finding is not observed in most of the cases. Venous thrombosis should be suspected in case of hemorrhage or edema near the dural venous sinus or deep cerebral vein. The most common direct sign on CTV is a filling defect in the dural venous sinus, also known as the "empty delta sign" (Poon et al. 2007). The sensitivity of CTV for detecting venous thromboses is higher for the dural venous sinuses than for the cortical veins. On the other hand, open dural sinuses appear as flow voids on MRI scans. Loss of flow void or abnormal signals imply thrombosis and detection would be more successful when imaging plane is perpendicular to the direction of blood flow. Signal intensity of the clot varies in time, similar to a hematoma, and should be confirmed with different sequences (Leach et al. 2006). SWI is highly beneficial in detecting subtle clots that are not visible with other sequences. MRV can detect a blood clot and help evaluate recanalization and collateral status with high accuracy (Fig. 11). Although TOF MRV does not require the use of a contrast agent (particularly important in patients with renal failure), which is an important advantage, it is necessary to be careful about pitfalls. Particularly on 2D TOF MRV, signal loss due to in-plane flow or hypoplastic/aplastic venous sinus can mimic thrombosis (Rollins et al. 2005). Filling defect can be directly visualized using postcontrast MRV. However, it should also be remembered that chronic thrombosis may exhibit contrast uptake on MRV, thereby leading to the interpretation of the sinus as normal, which is a false-negative result (Dmytriw et al. 2018).

3.2.3 Nontraumatic Subarachnoid Hemorrhage

The most common cause of subarachnoid hemorrhage (SAH) is trauma, whereas the most common cause of nontraumatic SAH is a ruptured aneurysm (nearly 85%). In addition to aneurysms, amyloid angiopathy, venous thrombosis, and vascular anomalies can also cause spontaneous SAH. Aneurysmal SAH is a very severe clinical presentation with a mortality rate ranging from 18% to 67% (Connolly et al. 2012; van Gijn et al. 2007). It also has high morbidity, wherein only one-third of the patients achieve full recovery after treatment. The classic clinical presentation of aneurysmal SAH is sudden onset of (within 1 min.) severe headache described as "the worst headache of my life" by the patients (Ducros and Bousser 2013). In addition, photophobia, seizures, vomiting, neck stiffness, and changes in consciousness can also be observed. The first imaging modality used in diagnosis is noncontrast CT. Lumbar puncture is recommended when noncontrast CT result is negative, for patients who are clinically suspected of having SAH (sudden onset and severe headache). Sensitivity of noncontrast CT for detecting SAH reaches up to 100% when performed within the first 6 h after the onset of symptoms (Carpenter et al. 2016; Perry et al. 2011). Sensitivity decreases with time and drops down to less than 90% within the first 72 h. Fissures and/or basal cisterns appear hyperdense on noncontrast CT scans. Pattern of bleeding provides information about the localization of the aneurysm. For instance, presence of blood in the interhemispheric fissure and lateral ventricle suggests anterior communicating artery aneurysm, whereas blood in the Sylvian fissure suggests middle cerebral artery aneurysm. Blood frequently extravasates to the brain parenchyma (30%) and ventricles (>50%) other than the subarachnoid space after the aneurysm ruptures, whereas subdural hemorrhage is rare (<5%). Vascular examination should be performed to determine the underlying cause after a patient has been diagnosed with SAH. DSA is the gold standard for determining the cause of hemorrhage and planning the treatment (Fig. 12). DSA is invasive, risky, and time-consuming; therefore, it has been replaced by CTA. Saccular aneurysms appear on CTA as round-shaped lesions filled with contrast forming a sac protruding from the vessel wall. Saccular aneurysms that cause SAH are fre-
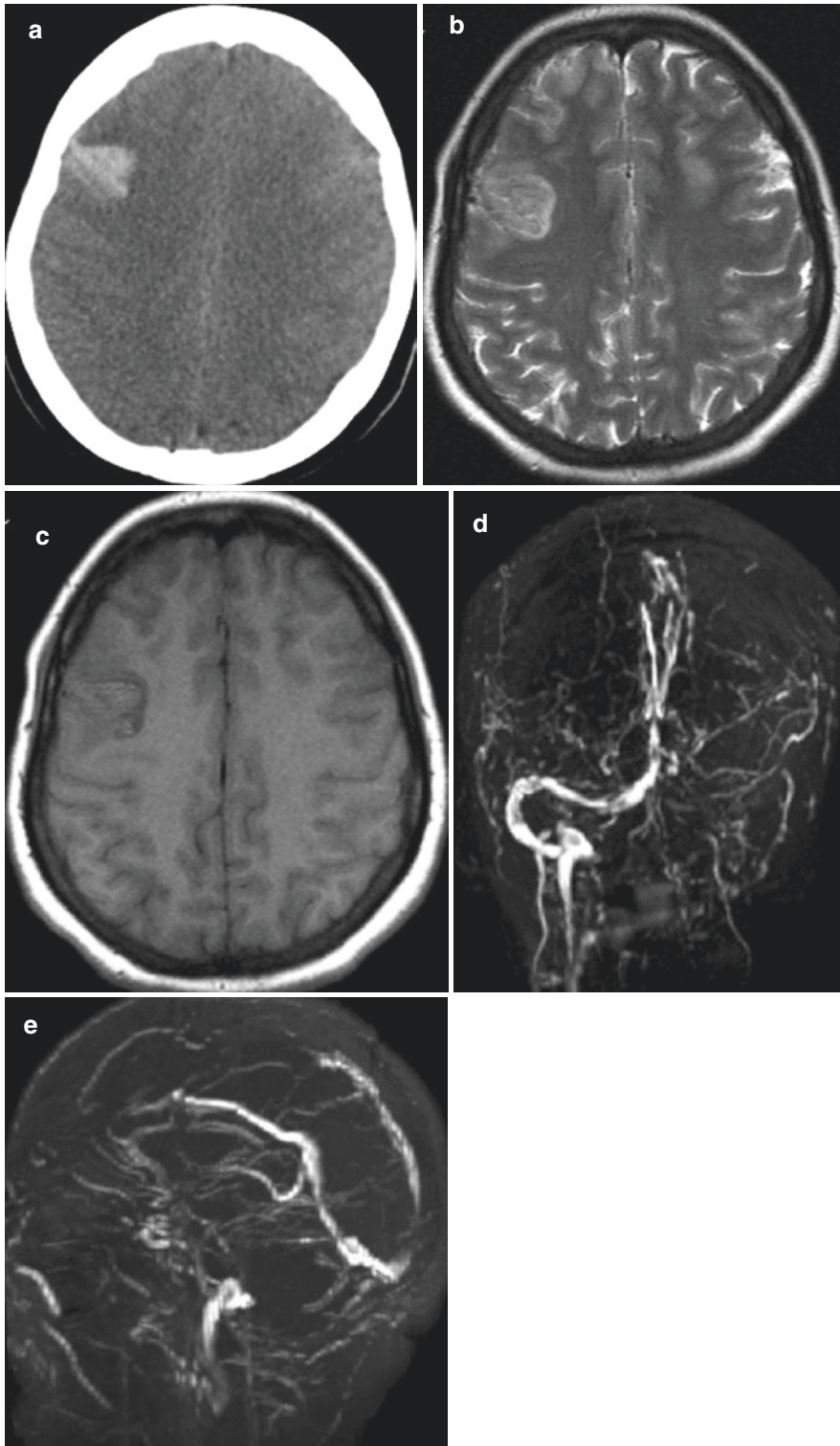
Fig. 11 Dural venous sinus thrombosis. (**a**) Noncontrast CT shows right frontal acute hematoma. (**b**, **c**) T2W and T1W images depict the hematoma as well as cortical thickening and edema on the left hemisphere. (**d**, **e**) MR venography shows partial occlusion of the superior sagittal sinus and total occlusion on the left transverse and sigmoid sinuses
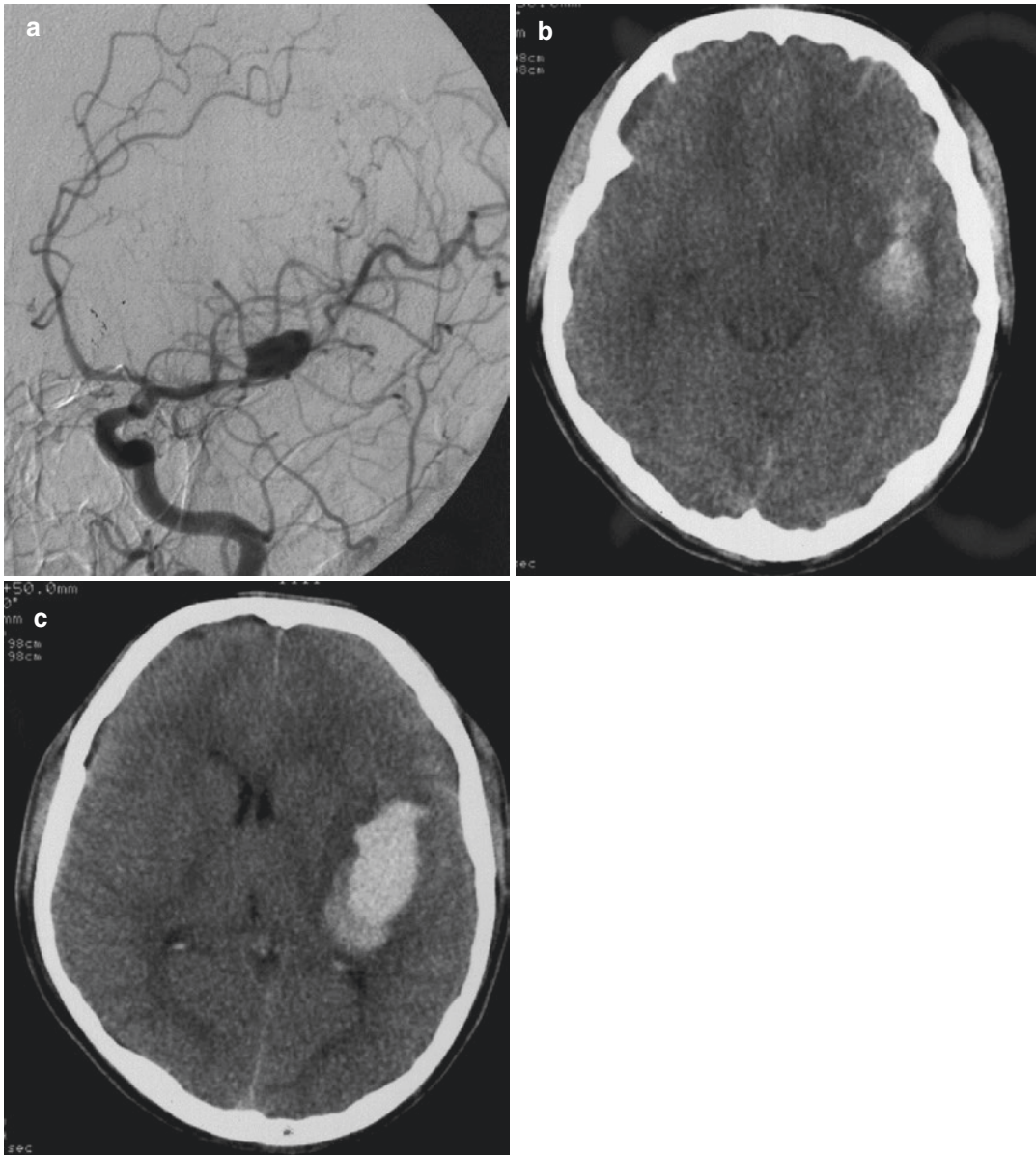
Fig. 12 Aneurysm. (**a**) DSA reveals an aneurysm on the left middle cerebral artery bifurcation which caused both intracerebral hematoma and subarachnoid hemorrhage on the left cerebral hemisphere (**b**, **c**)

quently localized at the bifurcation of major arteries in the Willis polygon. The risk of rupture is especially higher for aneurysms larger than 10 mm. DSA should be preferred when noncontrast CT and CTA are negative. CTA or DSA can be repeated or an MRI/MRA can be performed when DSA is also negative. However, the clinical presentation prevents performing an MRI in many patients. It was shown that aneurysms

could be detected in 10% of such patients, when DSA was repeated several weeks later. Increased cerebrospinal fluid (CSF) signal intensity on FLAIR is sensitive but not specific for SAH (Fig. 13). Conditions that cause sulcal hyperintensity on FLAIR are shown in Table 6.

Aneurysms are repaired using 2 methods: neurosurgical clipping or endovascular coiling. Endovascular coiling was shown to provide better
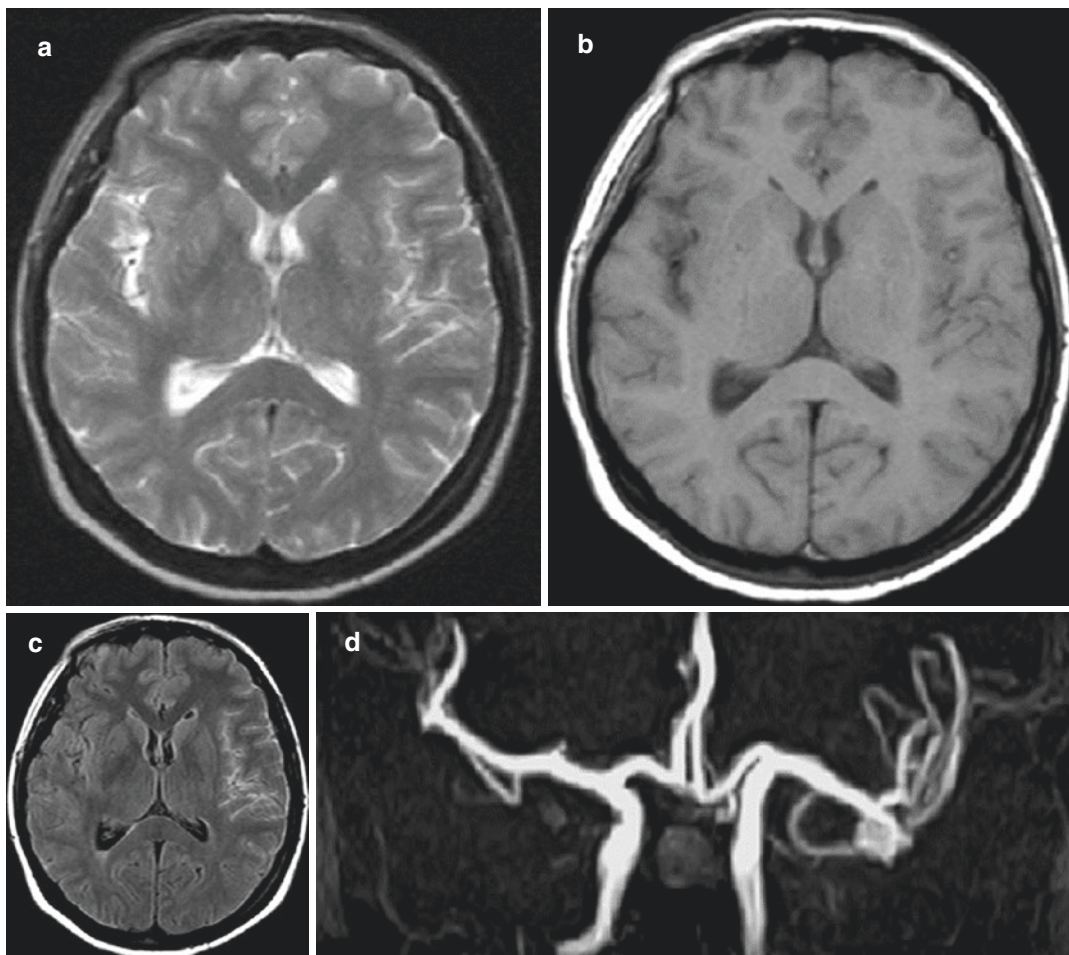
Fig. 13 Subarachnoid hemorrhage. (**a**, **b**) T2W and T1W images look normal whereas FLAIR image (**c**) depicts sulcal hyperintensity on the left hemisphere, consistent with SAH. (**d**) 3D TOF MRA shows left middle cerebral artery bifurcation aneurysm

Table 6 Differential diagnosis of subarachnoid FLAIR hyperintensity

Differential diagnosis of subarachnoid FLAIR hyperintensity
Subarachnoid hemorrhage
Meningitis
Leptomeningeal carcinomatosis
Leptomeningeal melanomatosis
Acute stroke
Moyamoya disease
Fat-containing lesions (lipoma, ruptured dermoid cyst)
Hyperoxygenation therapy
Artifacts (CSF flow artifact, magnetic susceptibility artifact, motion artifact, vascular pulsation artifact

outcomes. However, it is not possible to perform endovascular coiling in every patient. Treatment selection depends on the localization and size of the aneurysm, general condition of the patient, and experience of the clinician. The most severe complication of SAH is rebleeding, which is mostly seen within the first 6 h, with a mortality rate of 8–23% (Larsen and Astrup 2013). A late complication of SAH is cerebral vasospasm, which mostly occurs within the first 10 days and may lead to cerebral infarction. Incidence of cerebral vasospasm is directly proportional to the amount of blood in the subarachnoid space at the time of diagnosis.

3.2.4 Coagulopathy

Coagulopathies can be acquired (anticoagulants, idiopathic thrombocytopenic purpura, disseminated intravascular coagulation, alcoholism, etc.) or genetic (hemophilia A and B, von Willebrand factor deficiency, etc.). They account for 10–20% of all nontraumatic ICHs (Ciura and Romero 2014). Acquired coagulopathies constitute the majority of all coagulopathies. The epidemiology of the causes of ICH keeps changing due to the administration of more aggressive therapies for hypertension and increased use of anticoagulants, wherein the incidence of hemorrhages due to oral anticoagulant use is also increased (Flaherty et al. 2007). Currently, the most common cause of hemorrhages due to coagulopathy is medication.

It was proposed that anticoagulants alone did not cause ICH but increased the bleeding volume in patients who were predisposed to bleeding (e.g., CAA and hypertensive arteriopathy). Studies showed that hematoma expansion, hematoma volume, and mortality were higher in patients who used anticoagulants than those who did not (Horstmann et al. 2013; Flibotte et al. 2004). Nonoral anticoagulants pose a higher risk of ICH than oral anticoagulants. In addition, advanced age, hypertension, and use of multiple anticoagulants increase the risk of bleeding. While hemorrhages due to anticoagulants may have intraparenchymal, subdural, epidural, or subarachnoid localization, they most frequently have intraparenchymal and lobar localization. This reflects the probable contribution of CAA to the risk of intracerebral hemorrhage in the elderly.

3.2.5 Neoplasm

Hemorrhages associated with neoplasms constitute 10% of all ICHs. It was found in autopsy series that nearly half of all intracranial neoplasms exhibited histopathological bleeding. However, most microscopic bleeds do not manifest with clinical signs. Brain tumors that exhibit bleeding may be primary or metastatic tumors. The primary brain tumor that most frequently causes ICH is glioblastoma, and metastatic tumors that most frequently manifest with bleeding are bronchogenic carcinomas, choriocarcinoma, melanoma, thyroid carcinoma, and renal cell carcinoma. Tumors that cause bleeding are usually malignant. On the other hand, it should be remembered that benign tumors such as meningioma, pituitary adenoma, and vestibular schwannoma may also lead to ICH.

It is not always possible to show that a tumor is the underlying cause of hemorrhage on noncontrast CT. However, edema that is more than expected and rather heterogenous appearance of the hematoma should raise suspicion. Features that help differentiate intratumoral bleeding from primary ICH are more clearly visible on MRI. Hemorrhagic neoplasms appear more heterogenous than benign causes of bleeding due to the coexistence of blood products and tumor tissues (Destian et al. 1989). Another difference is observed in the amount of edema, mass effect, and persistence. Intratumoral hemorrhages exhibit more edema and mass effect and they persist for a long time or become worse. The hemosiderin ring around the hematoma is incomplete and irregular, and even not visible sometimes, in neoplastic hemorrhages (Atlas et al. 1987). In addition, in neoplasic hemorrhages, the expected signal change in the bleeding over time may prolong. Hypointensity observed on T2WI in the acute or early subacute phase may continue longer than 1 week. Postcontrast series are also highly beneficial in showing tumors that are the underlying cause of bleeding. Presence of contrast uptake in the nonhemorrhagic areas of the mass or observing multiple lesions particularly in metastatic disease is helpful for making a diagnosis (Fig. 14). Of note, subacute hematomas can also exhibit slight contrast uptake. However, contrast uptake due to neoplasms is more nodular and thicker. Sometimes a large hematoma or a small tumor makes it harder to visualize an underlying mass. MRI follow-up is recommended in such cases, if a tumor is suspected (e.g., large amount of edema and mass effect) (Ciura and Romero 2014).

3.2.6 Hemorrhagic Transformation of Ischemic Stroke

Hemorrhagic transformation of ischemic stroke refers to bleeding into the arterial infraction area.
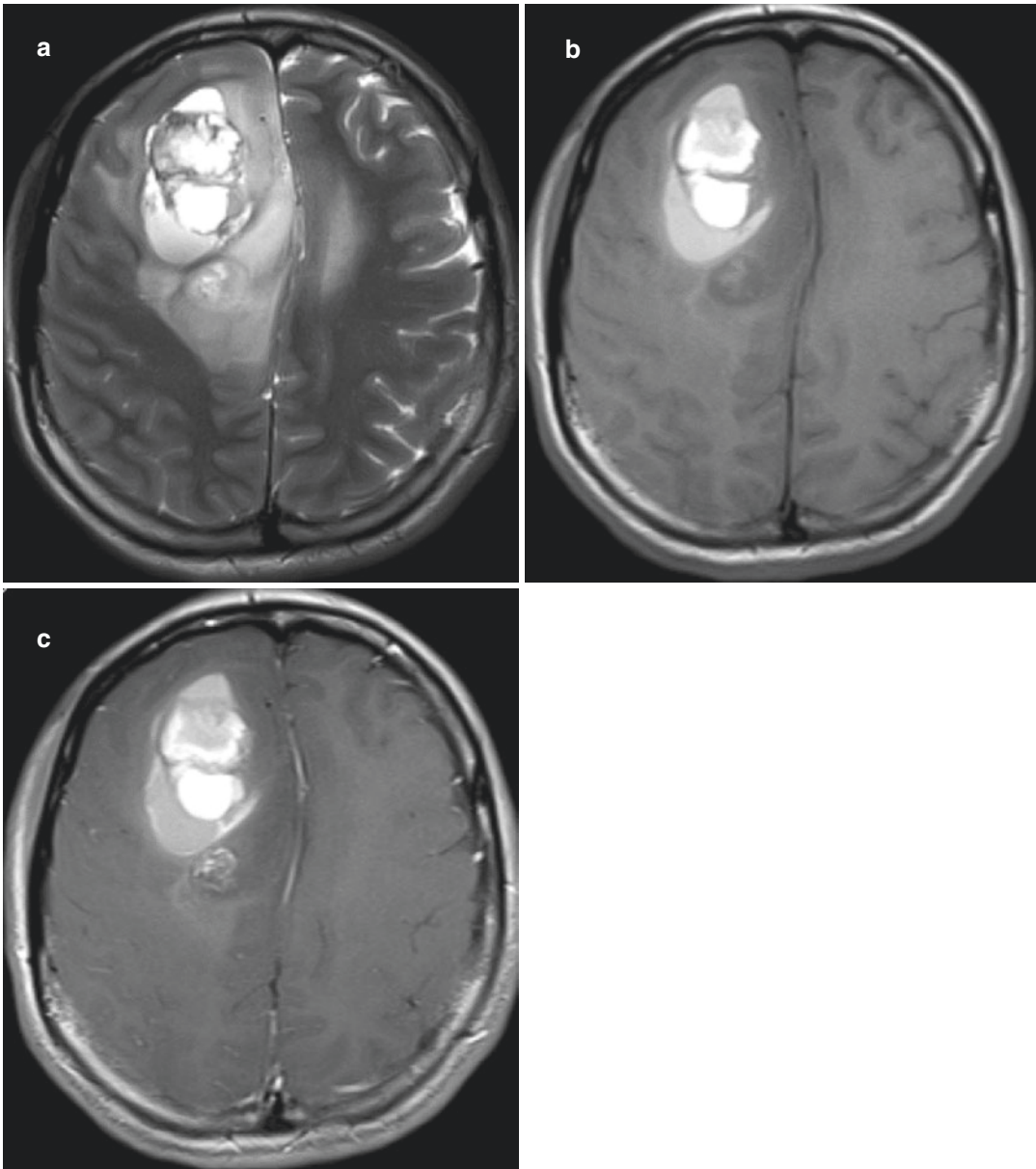
Fig. 14 Tumoral hemorrhage. A patient with bronchial carcinoma. (**a**, **b**) T2W and T1W images demonstrate a right frontal subacute hematoma with prominent periph-eral edema. (**c**) Postcontrast image depicts focal smaller enhancing lesion at the posterior aspect of the hematoma consistent with metastasis

One-third of all ischemic infarcts exhibit hemor-rhagic transformation (Hart and Easton 1986). One of the leading causes of hemorrhagic transfor-mation is thrombolytic therapy. 6–12% of the patients who receive thrombolytic therapy develop hemorrhagic transformation. Hemorrhagic trans-formation after thrombolytic therapy generally

occurs in the early phase (first 48 h), whereas spontaneous hemorrhages can be observed up to 2 weeks after ischemia. Apart from thrombolytic therapy, hypertension, hyperglycemia, use of oral anticoagulants, advanced age, and severe infarcts are other factors that lead to increased risk of hem-orrhagic transformation (Aviv et al. 2009;
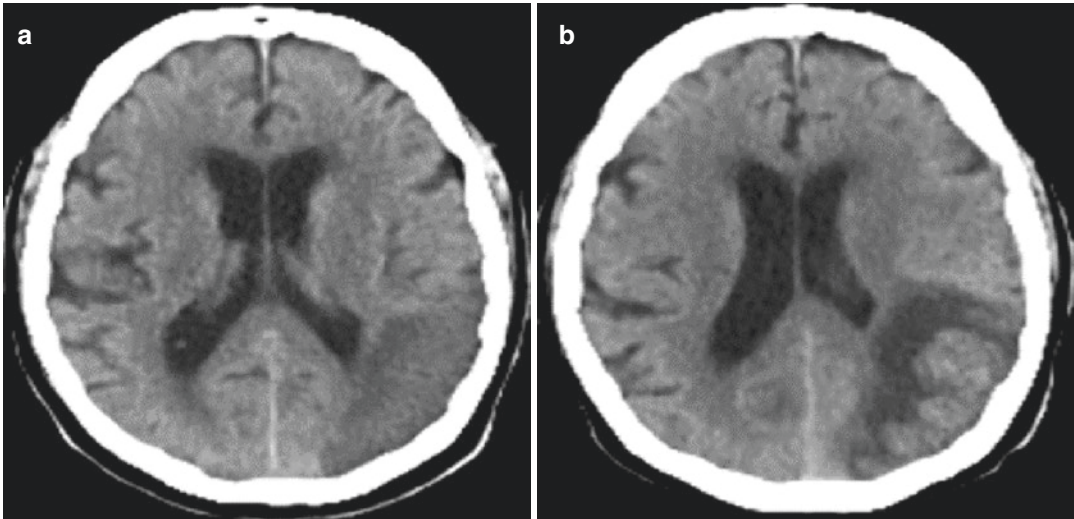
Fig. 15 (**a**) Noncontrast CT shows acute infarction at the posterior temporal lobe. (**b**) 3 days later, hyperdense areas consistent with hemorrhage occurred in the infarcted area. Hemorrhagic transformation

Lansberg et al. 2007a). Hemorrhage can be petechial or parenchymal. Petechial hemorrhages do not usually have a clinical sign; they are detected in imaging and create gyriform low signal on T2*-weighted sequences. CT findings are even more unspecific with punctate hyperdensities in gray matter. Parenchymal hemorrhages have a more severe clinical presentation. In case of parenchymal hemorrhage, it may be difficult to distinguish between hemorrhagic transformation of ischemic infarct and other causes of intraparenchymal hemorrhage. A large area of cytotoxic edema around the hematoma and signal change compatible with a specific arterial feeding area on CT and MRI should raise suspicion (Fig. 15). In addition, DWI and SWI are also highly beneficial in the diagnosis. It is important to demonstrate an infarct area with low ADC along with a low-signal bleeding area on SWI.

Imaging findings that reflect the risk of hemorrhage in patients with ischemic stroke have been defined. A large hypodense area that reflects the infarction area on CT, hyperdense middle cerebral artery (MCA) sign, and prolonged period between stroke onset and initial imaging were associated with a high risk of hemorrhage (Chen et al. 2016; Lansberg et al. 2007b). It was also shown that a high blood–brain barrier per-

meability and hypoperfusion status on perfusion CT were associated with hemorrhagic transformation (Suh et al. 2019). It was demonstrated that a higher baseline DWI lesion volume on MRI meant a higher risk of bleeding to the same extent (Lansberg et al. 2007a).

3.2.7 Vasculitis/Vasculopathy

Vasculitis is the inflammation of blood vessel walls. As a result of inflammation, the vessel wall becomes thicker, luminal narrowing, or occlusion occurs or the vessel ruptures due to necrosis of the blood vessel wall. Therefore, ischemic symptoms due to occlusion or ICH due to blood vessel rupture is observed in vasculitis. Nearly 11% of the patients with CNS vasculitis develop ICH. The hemorrhage is frequently parenchymal, but it can also have subarachnoid and rarely subdural localization (Rehman 2000).

Vasculitis is diagnosed based on clinical findings, laboratory tests, and radiologic imaging due to the challenges in biopsy. Patients usually present with nonspecific symptoms such as headache, seizures, and focal neurologic deficits. Increased sedimentation rate and elevated CRP values according to the laboratory tests suggest inflammation. Imaging findings can be direct or indirect in CNS vasculitis. Direct findings of vessel

involvement are thickening of the vessel wall and intramural contrast uptake, whereas indirect findings are luminal narrowing of the vessel and resulting ischemia, as well as perfusion abnormalities and ICH. The gold standard imaging modality in the diagnosis of CNS vasculitis is DSA. The specified inflammatory changes classically cause segmental cerebral vein stenosis and enlargement on angiography. However, the most commonly employed modality in patients with suspected vasculitis is MRI/MRA. The sensitivity of MRA for the diagnosis of large artery vasculitis reaches up to 100%, whereas DSA is superior to MRA in detecting pathologies of the small arteries (Pipitone et al. 2008; Garg 2011). Therefore, DSA should be performed when MRI + MRA is negative in patients suspected of having CNS vasculitis in order to rule out or diagnose small vessel involvement (Abdel Razek et al. 2014).

Moyamoya disease is a progressive vaso-occlusive disease of the distal internal carotid artery and its proximal branches (proximal anterior and middle cerebral arteries). As a result of occlusion, the lenticulostriate arteries and other perforating arteries become enlarged and form collateral vessel networks (puff of smoke). The term "Moyamoya syndrome" is used if there is an underlying cause (sickle cell anemia, neurofibromatosis type I, Down syndrome). MRI particularly shows ischemic lesions with watershed appearance and MRA shows lenticulostriate collateral veins and stenosis in the supraclinoid ICA. The disease generally manifests with cerebral ischemia in children, whereas hemorrhage is more prominent in the adult population. Hemorrhage is generally secondary to collateral vein rupture. Intraventricular hemorrhage is common, wherein intraparenchymal or subarachnoid hemorrhage can also be observed. Another cause of hemorrhage is the rupture of an anterior choroidal artery aneurysm, which is common in Moyamoya disease. The rate of rebleeding and infraction was shown to be higher in hemorrhage due to Moyamoya disease as compared to primary ICH (Nah et al. 2012).

Reversible cerebral vasoconstriction syndrome (RCVS) is characterized by thunderclap headache and manifests with vasoconstriction in multiple cerebral arteries. In addition, the patients may also have ischemic or hemorrhagic stroke and focal neurologic deficits. Vascular examination shows multifocal segmental constrictions in cerebral veins. Unlike other vasculopathies, these findings disappear within less than 3 months. Hemorrhages associated with RCVS can be isolated convexity SAH or intraparenchymal (Fig. 16). RCVS-associated hemorrhages were reported to be more prevalent in females and those with migraine type headaches (Ducros et al. 2010). Distinguishing RCVS from CNS vasculitis is essential for both administering the suitable treatment and predicting the prognosis. When RCVS is accurately diagnosed, unnecessary use of steroids and immunosuppressive agents, which are used to treat CNS vasculitis, would be prevented and the related side effects would be avoided. Elimination of the stimulus that triggers the syndrome would generally be sufficient to treat RCVS. In addition, compared to CNS vasculitis, RCVS does not require a biopsy to diagnose, the clinical picture is not progressive, and RCVS is more benign (Ducros et al. 2007; Marder et al. 2012).

3.2.8 Infection

Cerebral infections rarely cause ICH. However, it is critical to determine the infectious agent that causes ICH in order to start a specific treatment as soon as possible. Infectious agents cause hemorrhage via various mechanisms. These consist of vasculitis (as a result of the inflammatory reaction caused by the infectious agent on the vessel wall) and vessel wall necrosis, coagulopathy (thrombocytopenia, DIC, hemophagocytic syndrome), septic emboli, and microbial aneurysm rupture (Radwan and Sawaya 2011).

Infection should be considered, although rare, in the differential diagnosis of ICH in patients who do not have risk factors such as hypertension, who have negative angiography results and clinical (fever) and laboratory (leukocytosis, elevated sedimentation rate, and CRP) findings consistent with infection. CT and MRI may show bilateral multifocal hemorrhage foci secondary to septic emboli. Septic emboli should be suspected especially in the presence of bacterial endocarditis, miliary tuberculosis, and cryptococcal infec-
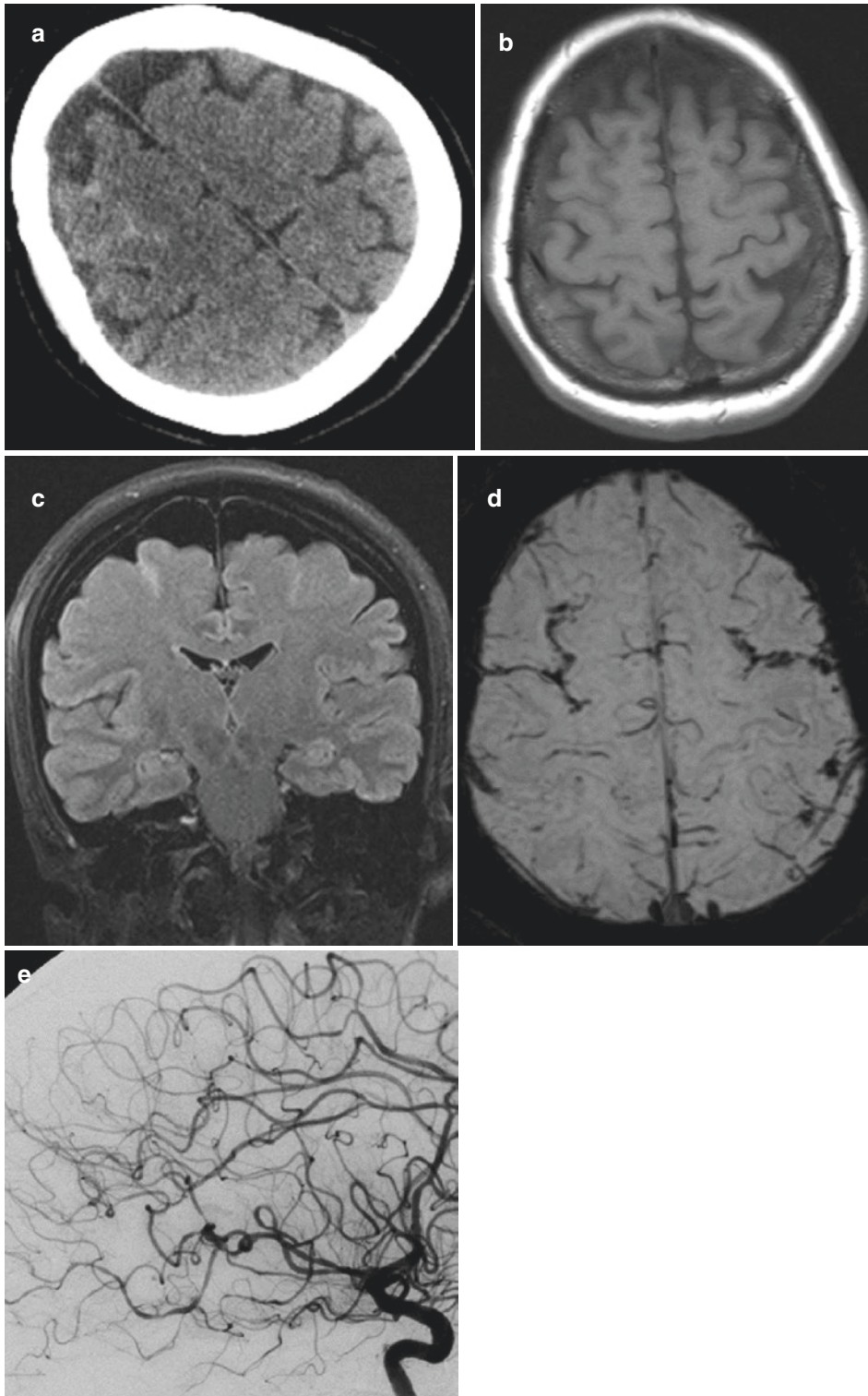
Fig. 16 RCVS. (**a**) Noncontrast CT shows right frontal sulcal SAH in a young woman. T1W image looks normal (**b**) whereas FLAIR image (**c**) demonstrates sulcal hyperintensity on the right frontal region. (**d**) SWI much better demonstrates SAH in bilateral frontal sulci as sulcal hypointensities. (**e**) DSA shows beaded appearance and multiple focal stenotic areas in the distal branches of anterior and middle cerebral arteries
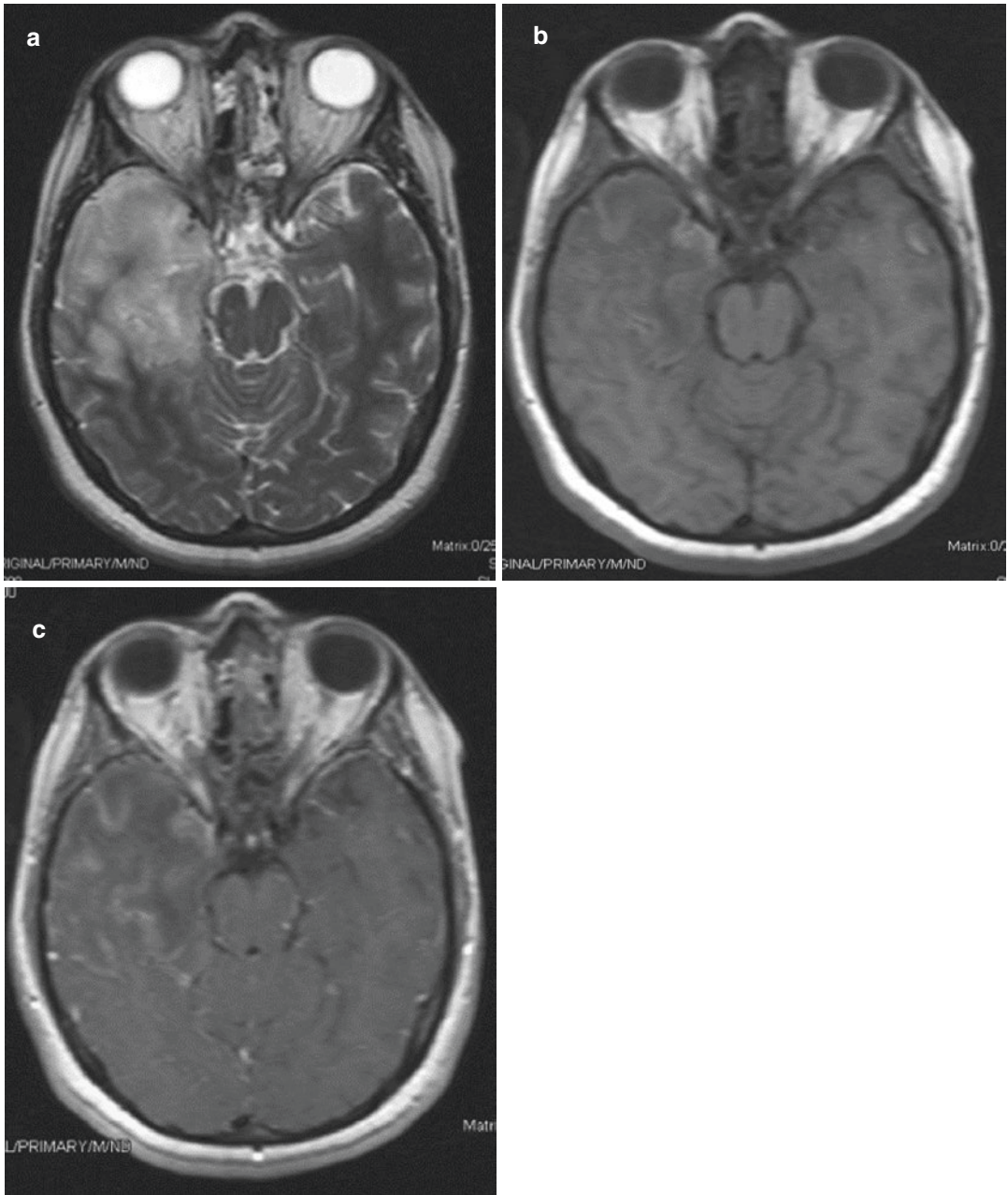
Fig. 17 Hemorrhagic infectious encephalitis. (**a**) T2W image displays hyperintense lesion on the right temporal lobe which is diagnosed as herpes encephalitis. (**b**) Noncontrast T1W image demonstrates hyperintense foci inside the lesion consistent with hemorrhage. (**c**) On postcontrast image, heterogenous enhancement of the lesion is depicted

tion. The agent that most frequently causes microbial aneurysms is *S. aureus*, which commonly affects the distal branches of the middle cerebral artery. Pathologically, vessel wall inflammation, destruction of the muscularis and elastic lamina, subintimal fibrosis, and intimal

hyperplasia can be observed. All these changes predispose the vein to rupture and SAH occurs. Herpes simplex virus (HSV) is the most common cause of encephalitis. HSV typically leads to necrotizing encephalitis that involves the temporal lobe, insula, and cingulate gyrus (Fig. 17).

Frequently, hemorrhage occurs secondary to necrosis. Hemorrhage is usually petechial. Intracranial hematoma formation is rarer (Argyriou et al. 2006). The mortality rate of HSV encephalitis ranges between 50 and 70%, wherein the prognosis is known to be worse in patients who have hemorrhage.

The most common causes of ICH in patients infected with HIV are neoplasms associated with HIV (primary CNS lymphoma, metastatic Kaposi's sarcoma) and opportunistic infections such as toxoplasmosis. However, ischemic lesions are more common than hemorrhages in patients with HIV (Pinto 1996).

3.2.9 Alcohol and Drugs

Alcohol is an important risk factor for ICH, and the risk is directly proportional to the amount of alcohol consumed. People who consume more than 40 g of alcohol per day (1 drink is defined as 12 g of alcohol) have a 4.6-fold increased risk of ICH in comparison with nondrinkers (Juvela et al. 1995). The risk increases up to 11.3-fold if alcohol consumption exceeds 120 g/day. ICH related to alcohol consumption is probably associated with the chronic increase in blood pressure due to alcohol. In addition, impaired hemostasis, decreased circulating levels of clotting factors produced by the liver, and DIC are other mechanisms that contribute to the pathophysiology of ICH. Hemorrhages may have intraparenchymal or subarachnoid localization (O'Connor et al. 2005).

Hemorrhages linked to drug abuse frequently occur due to sympathomimetic drugs (cocaine and amphetamine). Less frequently, opioids and cannabis may also cause ICH. Sympathomimetic drugs, especially cocaine and amphetamine, lead to a 9.6-fold increased risk of hemorrhage (Petitti et al. 1998). Whether the stroke is ischemic or hemorrhagic depends on the form of cocaine used. The hydrochloride form is more closely associated with hemorrhagic stroke and ICH than the alkaloidal form. In addition, it was shown that 41% of the patients with ICH associated with drug abuse also had coexisting pathologies such as an underlying aneurysm or AVM (Levine et al. 1991). Therefore, an angiography should be performed to detect underlying vascular malforma-

tions in drug users. In ICH associated with drug abuse, acute increase in blood pressure leads to hemorrhage unlike in the case of alcohol use. Moreover, cocaine is thought to cause hemorrhage by triggering the development of cerebral vasculitis or hemorrhagic transformation of ischemic infarct. It was shown that ICHs associated with cocaine use frequently had subcortical localization and more frequently had intraventricular extension and a poor prognosis.

References

Abdel Razek AA, Alvarez H, Bagg S, Refaat S, Castillo M (2014) Imaging spectrum of CNS vasculitis. Radiographics 34:873–894

Al-Shahi R, Warlow C (2001) A systematic review of the frequency and prognosis of arteriovenous malformations of the brain in adults. Brain 124:1900e26

Argyriou A, Tsota I, Solomou E, Marangos M, Kalogeropoulou C, Petsas T et al (2006) Intracerebral haemorrhage as a rare complication of HSV-1 meningoencephalitis: case report and review of the literature. Scand J Infect Dis 1:63–66

Atlas SW, Grossman RI, Gomori JM et al (1987) Hemorrhagic intracranial malignant neoplasms: spin-echo MR imaging. Radiology 164:71–77

Aviv RI, D'Esterre CD, Murphy BD et al (2009) Hemorrhagic transformation of ischemic stroke: prediction with CT perfusion. Radiology 250:867e77

Bejot Y, Cordonnier C, Durier J et al (2013) Intracerebral haemorrhage profiles are changing: results from the Dijon population-based study. Brain 136:658–664

Borden JA, Wu JK, Shucart WA (1995) A proposed classification for spinal and cranial dural arteriovenous fistulous malformations and implications for treatment. J Neurosurg 82:166–179

Brott T, Broderick J, Kothari R et al (1997) Early hemorrhage growth in patients with intracerebral hemorrhage. Stroke 28:1e5

Carpenter CR, Hussain AM, Ward MJ et al (2016) Spontaneous subarachnoid hemorrhage: a systematic review and meta-analysis describing the diagnostic accuracy of history, physical examination, imaging, and lumbar puncture with an exploration of test thresholds. Acad Emerg Med 23:963–1003

Chen G, Wang A, Zhao X, Wang C, Liu L, Zheng H, Wang Y, Cao Y, Wang Y (2016) Frequency and risk factors of spontaneous hemorrhagic transformation following ischemic stroke on the initial brain CT or MRI: data from the China National Stroke Registry (CNSR). Neurol Res 38:538–544

Ciura VA, Romero JM (2014) Nontraumatic acute intraparenchymal hemorrhage: algorithm for workup and differential diagnosis. Semin Roentgenol 49:112–126

Cognard C, Gobin YP, Pierot L et al (1995) Cerebral dural arteriovenous fistulas: clinical and angiographic correlation with a revised classification of venous drainage. Radiology 194:671–680

Connolly ES, Rabinstein AA, Carhuapoma JR et al (2012) Guidelines for the management of aneurysmal subarachnoid hemorrhage: a guideline for healthcare professionals from the American Heart Association/American Stroke Association. Stroke 43:1711–1737

Coutinho JM, Zuurbier SM, Aramideh M, Stam J (2012) The incidence of cerebral venous thrombosis: a cross-sectional study. Stroke 43:3375–3377

Delcourt C, Huang Y, Arima H, Chalmers J, Davis SM, Heeley EL et al (2012) Hematoma growth and outcomes in intracerebral hemorrhage: the INTERACT1 study. Neurology 79:314–319

Demchuk AM, Dowlatshahi D, Rodriguez-Luna D et al (2012) Prediction of haematoma growth and outcome in patients with intracerebral haemorrhage using the CT-angiography spot sign (PREDICT): a prospective observational study. Lancet Neurol 11:307–314

Destian S, Sze G, Krol G et al (1989) MR imaging of hemorrhagic intracranial neoplasms. Am J Roentgenol 152:137–144

Dmytriw AA, Song JSA, Yu E, Poon CS (2018) Cerebral venous thrombosis: state of the art diagnosis and management. Neuroradiology 60:669–685

Ducros A, Bousser MG (2013) Thunderclap headache. BMJ 346:e8557

Ducros A, Boukobza M, Porcher R et al (2007) The clinical and radiological spectrum of reversible cerebral vasoconstriction syndrome. A prospective series of 67 patients. Brain 130:3091–3101

Ducros A, Fiedler U, Porcher R et al (2010) Hemorrhagic manifestations of reversible cerebral vasoconstriction syndrome: frequency, features, and risk factors. Stroke 41:2505–2511

Ferro JM, Canhao P, Stam J et al (2004) Prognosis of cerebral vein and dural sinus thrombosis: results of the International Study on Cerebral Vein and Dural Sinus Thrombosis (ISCVT). Stroke 35:664e70

Fisher CM (1971) Pathological observations in hypertensive cerebral hemorrhage. J Neuropathol Exp Neurol 30:536–550

Flaherty ML, Kissela B, Woo D et al (2007) The increasing incidence of anticoagulant-associated intracerebral hemorrhage. Neurology 68:116–121

Flibotte JJ, Hagan N, O'donnell J et al (2004) Warfarin, hematoma expansion, and outcome of intracerebral hemorrhage. Neurology 63:1059–1064

Foulkes MA, Wolf PA, Price TR, Mohr JP, Hier DB (1988) The stroke data Bank: design, methods, and baseline characteristics. Stroke 19:547–554

Fujii Y, Takeuchi S, Sasaki O et al (1998) Multivariate analysis of predictors of hematoma enlargement in spontaneous intracerebral hemorrhage. Stroke 29:1160–1166

Garg A (2011) Vascular brain pathologies. Neuroimaging Clin N Am 21:897–926

Greenberg SM, Eng JA, Ning M, Smith EE, Rosand J (2004) Hemorrhage burden predicts recurrent intracerebral hemorrhage after lobar hemorrhage. Stroke 35:1415–1420

Gross BA, Du R (2017) Hemorrhage from cerebral cavernous malformations: a systematic pooled analysis. J Neurosurg 126:1079–1087

Haacke EM, Mittal S, Wu Z, Neelavalli J, Cheng YC (2009) Susceptibility-weighted imaging: technical aspects and clinical applications, part 1 AJNR. Am J Neuroradiol 30:19–30

Hart RG, Easton JD (1986) Hemorrhagic infarcts. Stroke 17:586–589

Hemphill JC 3rd, Greenberg SM, Anderson CS et al (2015) Guidelines for the management of spontaneous intracerebral hemorrhage: a guideline for healthcare professionals from the American Heart Association/American Stroke Association. Stroke 46:2032–2060

Horstmann S, Rizos T, Lauseker M et al (2013) Intracerebral hemorrhage during anticoagulation with vitamin K antagonists: a consecutive observational study. J Neurol 260:2046–2051

Juvela S, Hillbom M, Palomaki H (1995) Risk factors for spontaneous intracerebral hemorrhage. Stroke 26:1558–1564

Kidwell CS, Chalela JA, Saver JL et al (2004) Comparison of MRI and CT for detection of acute intracerebral hemorrhage. J Am Med Assoc 292:1823–1830

Knudsen KA, Rosand J, Karluk D et al (2001) Clinical diagnosis of cerebral amyloid angiopathy: validation of the Boston criteria. Neurology 56(4):539

Kreel L, Kay R, Woo J, Wong HY, Nicholls MG (1991) The radiological (CT) and clinical sequelae of primary intracerebral haemorrhage. Br J Radiol 64:1096–1100

Kumral E, Polat F, Uzunkopru C, Calli C, Kitis O (2012) The clinical spectrum of intracerebral hematoma, hemorrhagic infarct, non-hemorrhagic infarct, and non-lesional venous stroke in patients with cerebral sinus-venous thrombosis. Eur J Neurol 19:537–543

Lansberg MG, Thijs VN, Bammer R et al (2007a) Risk factors of symptomatic intracerebral hemorrhage after tPA therapy for acute stroke. Stroke 38:2275e8

Lansberg MG, Albers GW, Wijman CA (2007b) Symptomatic intracerebral hemorrhage following thrombolytic therapy for acute ischemic stroke: a review of the risk factors. Cerebrovasc Dis 24:1e10

Larsen CC, Astrup J (2013) Rebleeding after aneurysmal subarachnoid hemorrhage: a literature review. World Neurosurg 79:307–312

Leach JL, Fortuna RB, Jones BV, Gaskill-Shipley MF (2006) Imaging of cerebral venous thrombosis: current techniques, spectrum of findings, and diagnostic pitfalls. Radiographics 26:S19–S41

Levine SR, Brust JC, Futrell N et al (1991) A comparative study of the cerebrovascular complications of cocaine: alkaloidal versus hydrochloride—a review. Neurology 41:1173–1177

Lucas Cde P, Caldas JG, Prandini MN (2006) Do leptomeningeal venous drainage and dysplastic venous dilation predict hemorrhage in dural arteriovenous fistula? Surg Neurol 66(Suppl 3):S2–S5. discussion S5-6

Maia LF, Mackenzie IR, Feldman HH (2007) Clinical phenotypes of cerebral amyloid angiopathy. J Neurol Sci 257:23–30

Marder CP, Donohue MM, Weinstein JR et al (2012) Multimodal imaging of reversible cerebral vasoconstriction syndrome: a series of 6 cases. AJNR Am J Neuroradiol 33:1403–1410

Nah HW, Kwon SU, Kang DW et al (2012) Moyamoya disease-related versus primary intracerebral: hemorrhage location and outcomes are different. Stroke 43:1947–1950

Newton TH, Cronqvist S (1969) Involvement of dural arteries in intracranial arteriovenous malformations. Radiology 93:1071–1078

O'Connor AD, Rusyniak DE, Bruno A (2005) Cerebrovascular and cardiovascular complications of alcohol and sympathomimetic drug abuse. Med Clin North Am 89:1343–1358

Osborn AG (1994) Diagnostic neuroradiology. Mosby, St. Louis, MO

Pantoni L (2010) Cerebral small vessel disease: from pathogenesis and clinical characteristics to therapeutic challenges. Lancet Neurol 9:689–701

Perry JJ, Stiell IG, Sivilotti ML et al (2011) Sensitivity of computed tomography performed within six hours of onset of headache for diagnosis of subarachnoid haemorrhage: prospective cohort study. BMJ 343: d4277

Petitti DB, Sidney S, Quesenberry C et al (1998) Stroke and cocaine or amphetamine use. Epidemiology 9:596–600

Pinto AN (1996) AIDS and cerebrovascular disease. Stroke 27:538–543

Pipitone N, Versari A, Salvarani C (2008) Role of imaging studies in the diagnosis and follow-up of large-vessel vasculitis: an update. Rheumatology (Oxford) 47:403–408

Poon CS, Chang J-K, Swarnkar A, Johnson MH, Wasenko J (2007) Radiologic diagnosis of cerebral venous thrombosis: pictorial review. Am J Roentgenol 189:S64–S75

Radwan W, Sawaya R (2011) Intracranial haemorrhage associated with cerebral infections: a review. Scand J Infect Dis 43:675–682

Rammos S, Maina R, Lanzino G (2009) Developmental venous anomalies: current concepts and implications for management. Neurosurgery 65:20e9

Rehman HU (2000) Primary angiitis of the central nervous system. J R Soc Med 93:586–588

Rollins N, Ison C, Reyes T, Chia J (2005) Cerebral MR venography in children: comparison of 2D time-of-flight and gadolinium enhanced 3D gradient-echo techniques. Radiology 235:1011–1017

Romero JM, Artunduaga M, Forero NP et al (2009) Accuracy of CT angiography for the diagnosis of vascular abnormalities causing intraparenchymal hemorrhage in young patients. Emerg Radiol 16:195–201

Rosand J, Hylek EM, O'Donnell HC et al (2000) Warfarin associated hemorrhage and cerebral amyloid angiopathy: a genetic and pathologic study. Neurology 55:947e51

Saposnik G, Barinagarrementeria F, Brown RD, Bushnell CD, Cucchiara B, Cushman M, deVeber G, Ferro JM, Tsai FY (2011) On behalf of the American Heart Association stroke council and the council on epidemiology and prevention. Diagnosis and management of cerebral venous thrombosis: a statement for healthcare professionals from the American Heart Association/American Stroke Association. Stroke 42:1158–1192

Shahi R, Warlow C (2001) A systematic review of the frequency and prognosis of arteriovenous malformations of the brain in adults. Brain 124:1900e26

Smith EE, Nandigam KR, Chen YW et al (2010) MRI markers of small vessel disease in lobar and deep hemispheric intracerebral hemorrhage. Stroke 41:1933–1938

Spetzler RF, Martin NA (1986) A proposed grading system for arteriovenous malformations. J Neurosurg 65:476e83

Stapf C, Mast H, Sciacca R et al (2006) Predictors of hemorrhage in patients with untreated brain arteriovenous malformation. Neurology 66:1350e5

Suh CH, Jung SC, Cho SJ, Kim D, Lee JB, Woo DC, Oh WY, Lee JG, Kim KW (2019) Perfusion CT for prediction of hemorrhagic transformation in acute ischemic stroke: a systematic review and meta-analysis. Eur Radiol 29:4077–4087

Tanskanen M, Makela M, Myllykangas L et al (2012) Prevalence and severity of cerebral amyloid angiopathy: a population-based study on very elderly Finns (Vantaa 85+). Neuropathol Appl Neurobiol 38:329–336

Tsai LK, Jeng JS, Liu HM et al (2004) Intracranial dural arteriovenous fistulas with or without cerebral sinus thrombosis: analysis of 69 patients. J Neurol Neurosurg Psychiatry 75:1639–1641

van Asch CJ, Luitse MJ, Rinkel GJ et al (2010) Incidence, case fatality, and functional outcome of intracerebral haemorrhage over time, according to age, sex, and ethnic origin: a systematic review and meta-analysis. Lancet Neurol 9:167–176

van Gijn J, Kerr R, Rinkel G (2007) Subarachnoid haemorrhage. Lancet 369:306–318

Wada R, Aviv RI, Fox AJ et al (2007) CT angiography "spot sign" predicts hematoma expansion in acute intracerebral hemorrhage. Stroke 38:1257–1262

Wycliffe ND, Choe J, Holshouser B et al (2004) Reliability in detection of hemorrhage in acute stroke by a new three-dimensional gradient recalled echo susceptibility-weighted imaging technique compared to computed tomography: a retrospective study. J Magn Reson Imaging 20:372–377

Xhu XL, Chan MS, Poon WS (1997) Spontaneous intracranial hemorrhage: which patients need diagnostic cerebral angiography? Stroke 28:1406–1409

Yeung R, Ahmad T, Aviv RI et al (2009) Comparison of CTA to DSA in determining the etiology of spontaneous ICH. Can J Neurol Sci 36:176–180

Zipfel GJ, Shah MN, Refai D et al (2009) Cranial dural arteriovenous fistulas: modification of angiographic classification scales based on new natural history data. Neurosurg Focus 26:E14